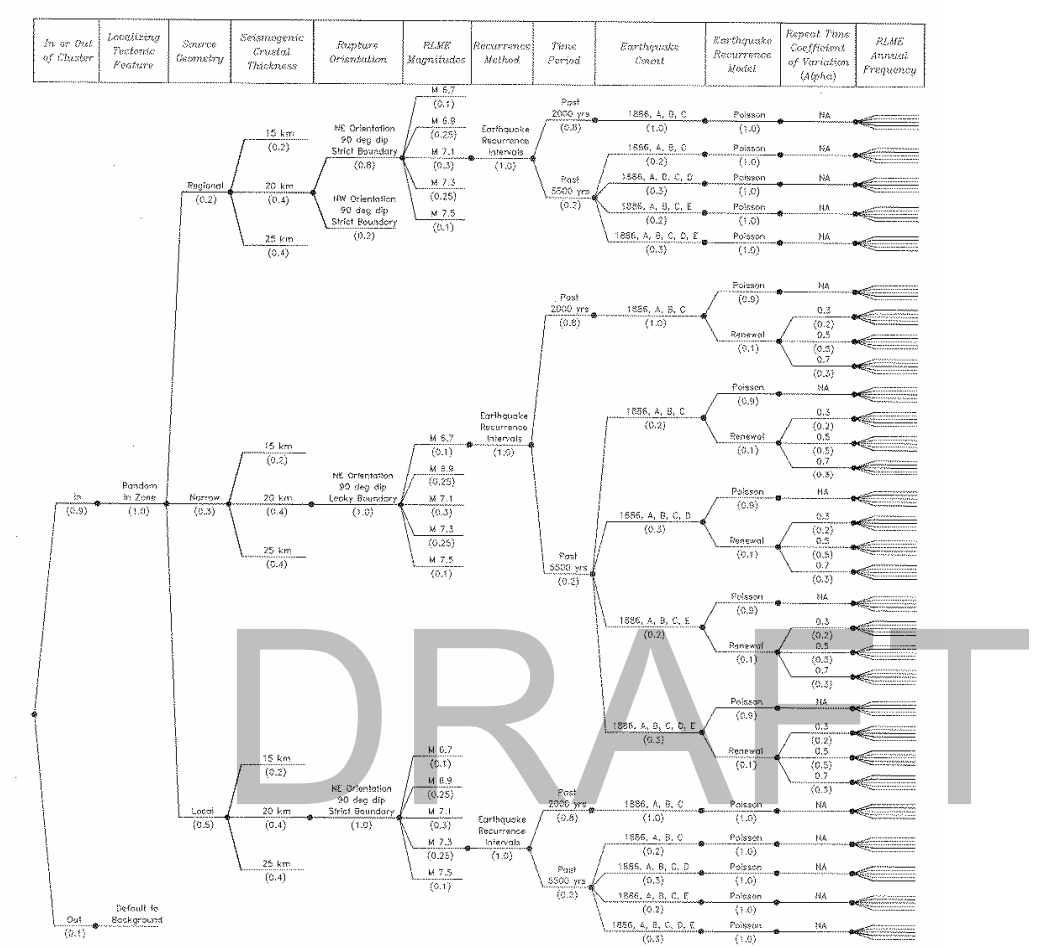

Figure 2.5.2-322: CEUS SSC model logic tree for the Charleston RLME source

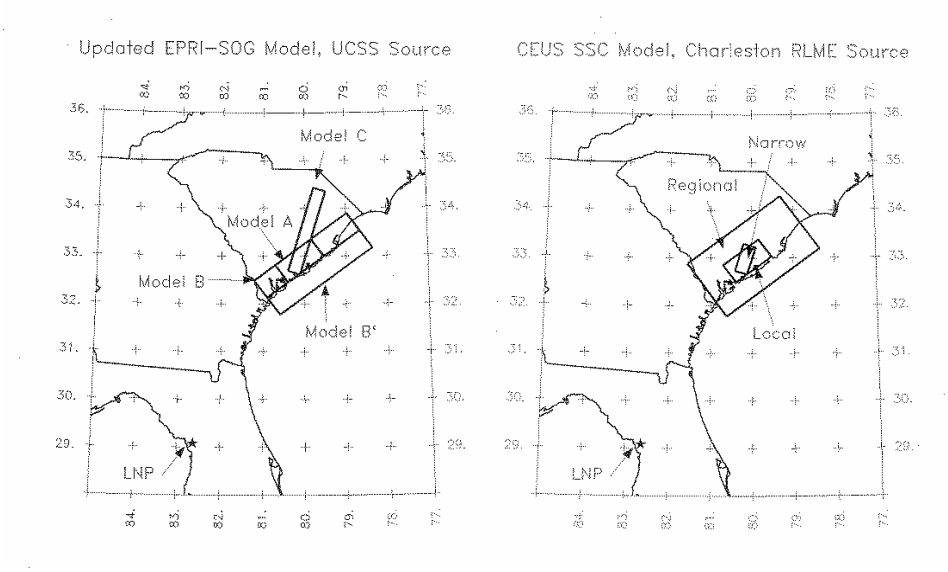

Figure 2.5.2-323: Alternative Charleston source geometries for the Charleston source.

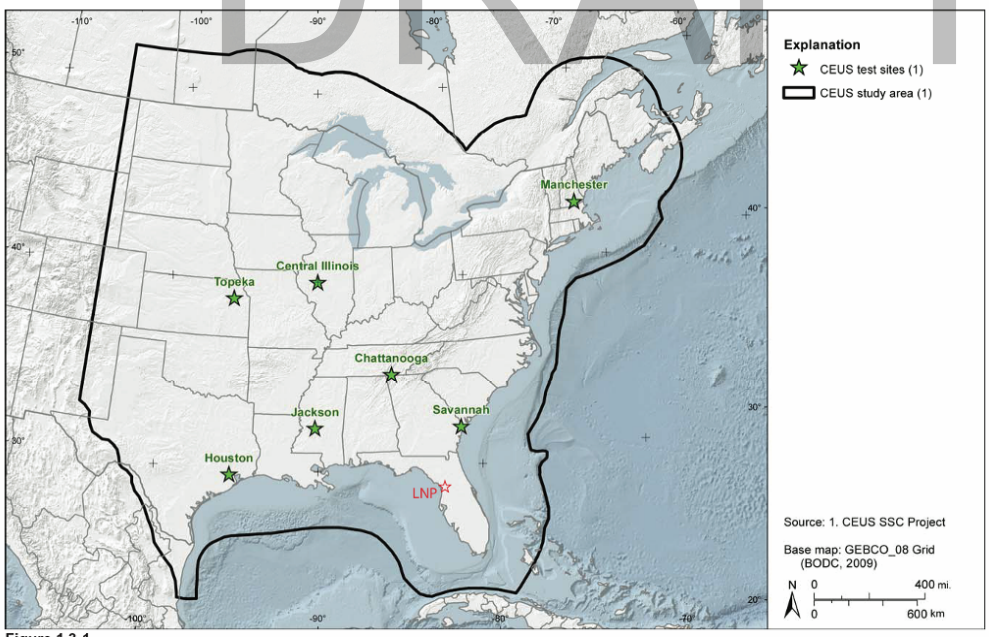

Figure 2.5.2-324: Location of seven demonstration sites used for hazard calculations in NUREG-2115 and the location of the LNP site. Approximate location of the LNP site is shown by the red star.

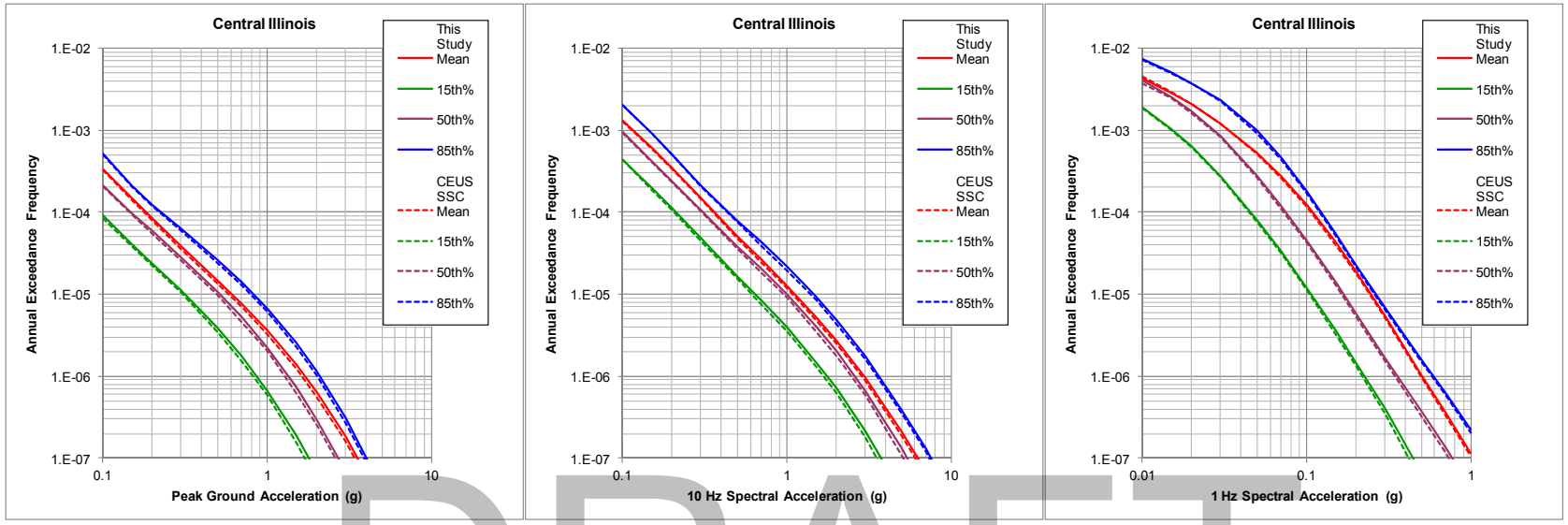

Figure 2.5.2-325: Comparison of hazard curves computed using AMEC E&I software with those listed in Chapter 8 of NUREG-2115 for the Central Illinois demonstration site

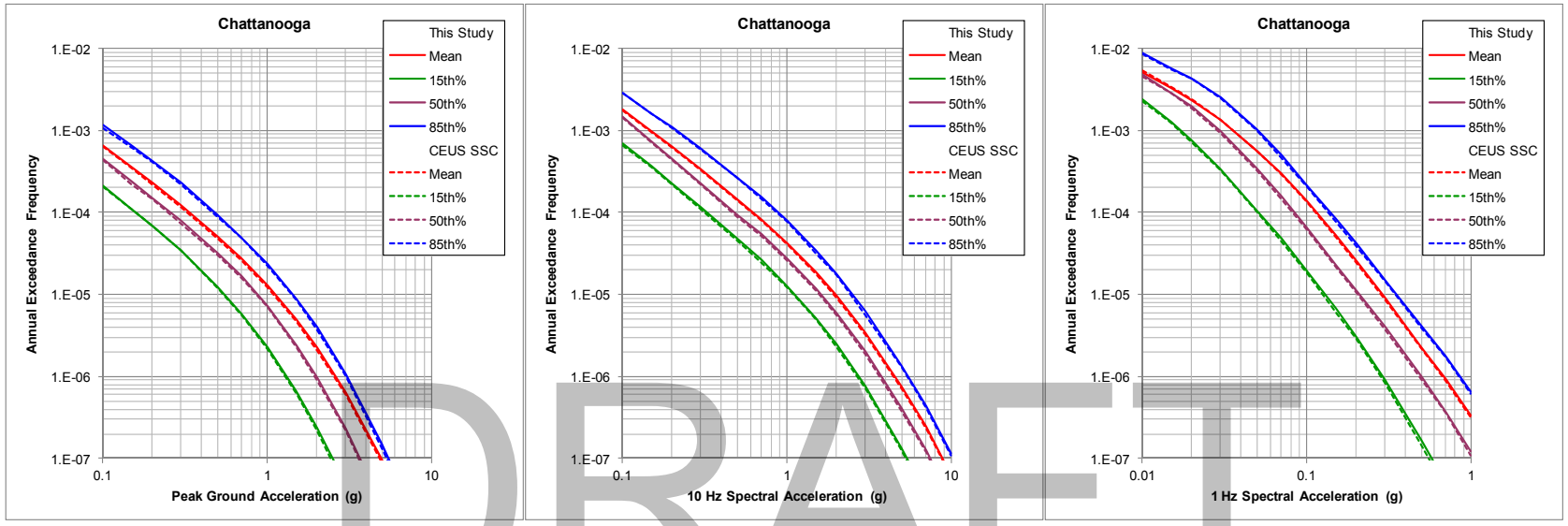

Figure 2.5.2-326: Comparison of hazard curves computed using AMEC E&I software with those listed in Chapter 8 of NUREG-2115 for the Chattanooga demonstration site

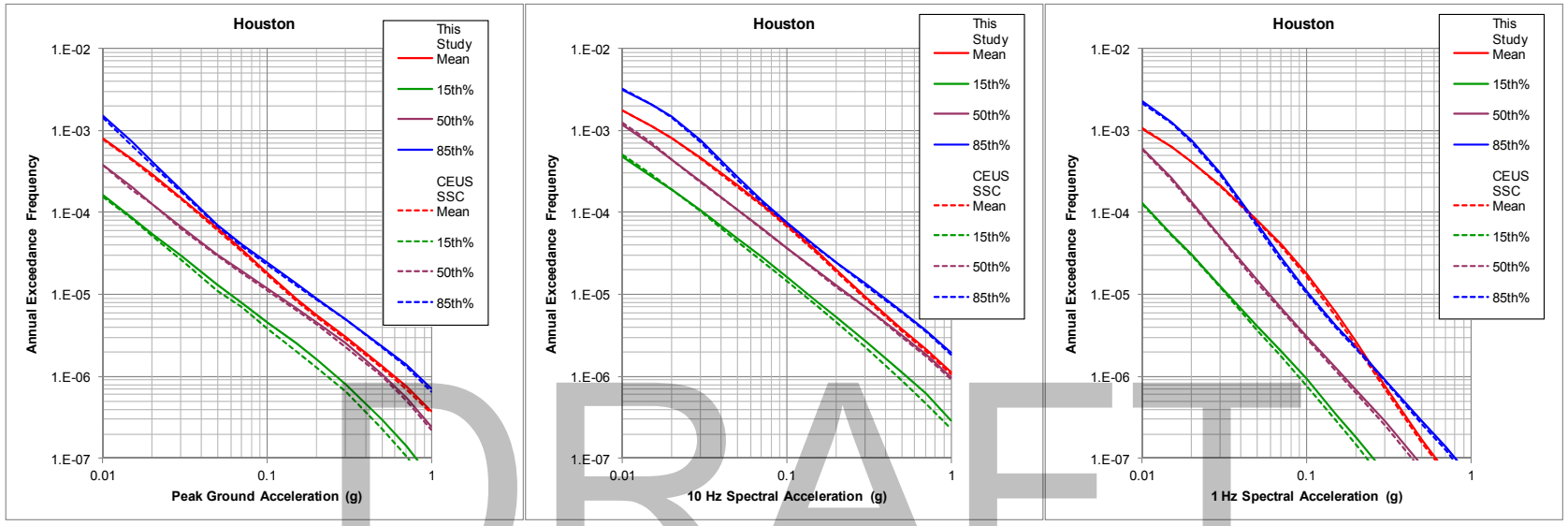

Figure 2.5.2-327: Comparison of hazard curves computed using AMEC E&I software with those listed in Chapter 8 of NUREG-2115 for the Houston demonstration site

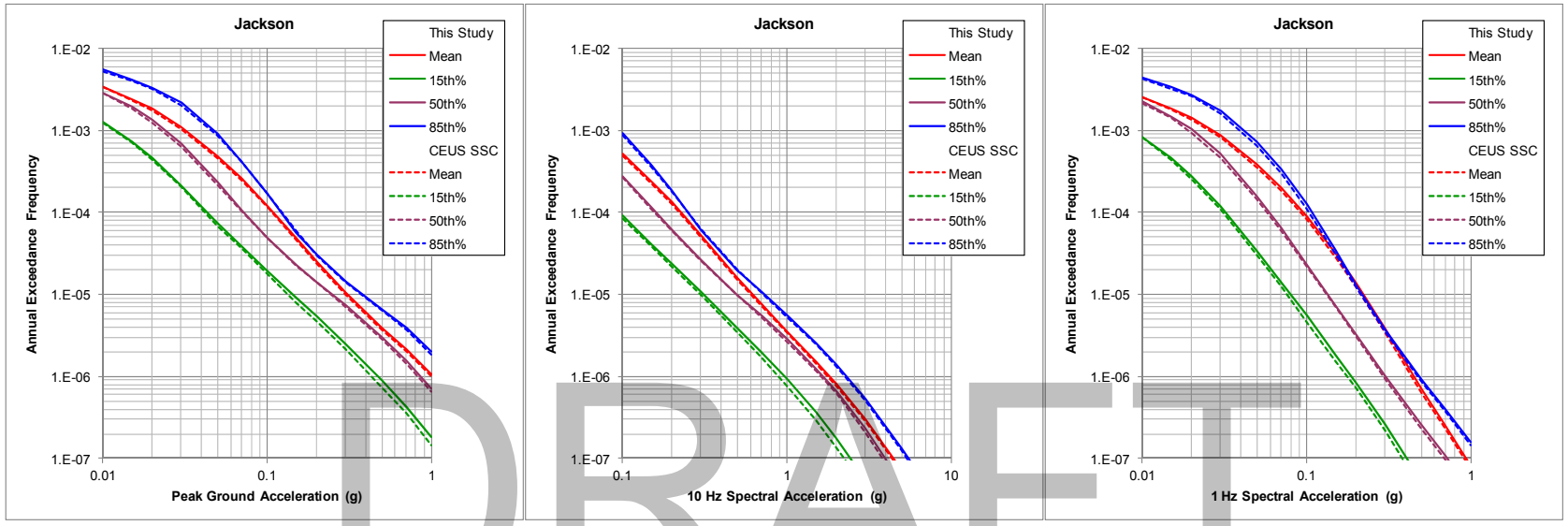

Figure 2.5.2-328: Comparison of hazard curves computed using AMEC E&I software with those listed in Chapter 8 of NUREG-2115 for the Jackson demonstration site

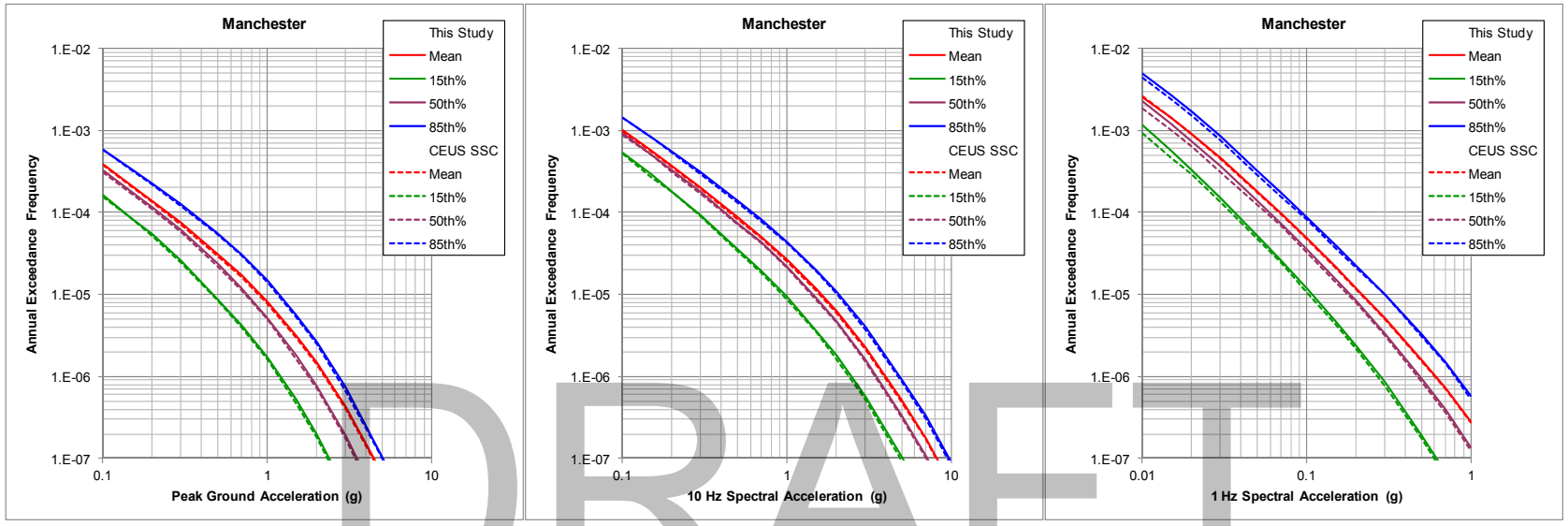

Figure 2.5.2-329: Comparison of hazard curves computed using AMEC E&I software with those listed in Chapter 8 of NUREG-2115 for the Manchester demonstration site

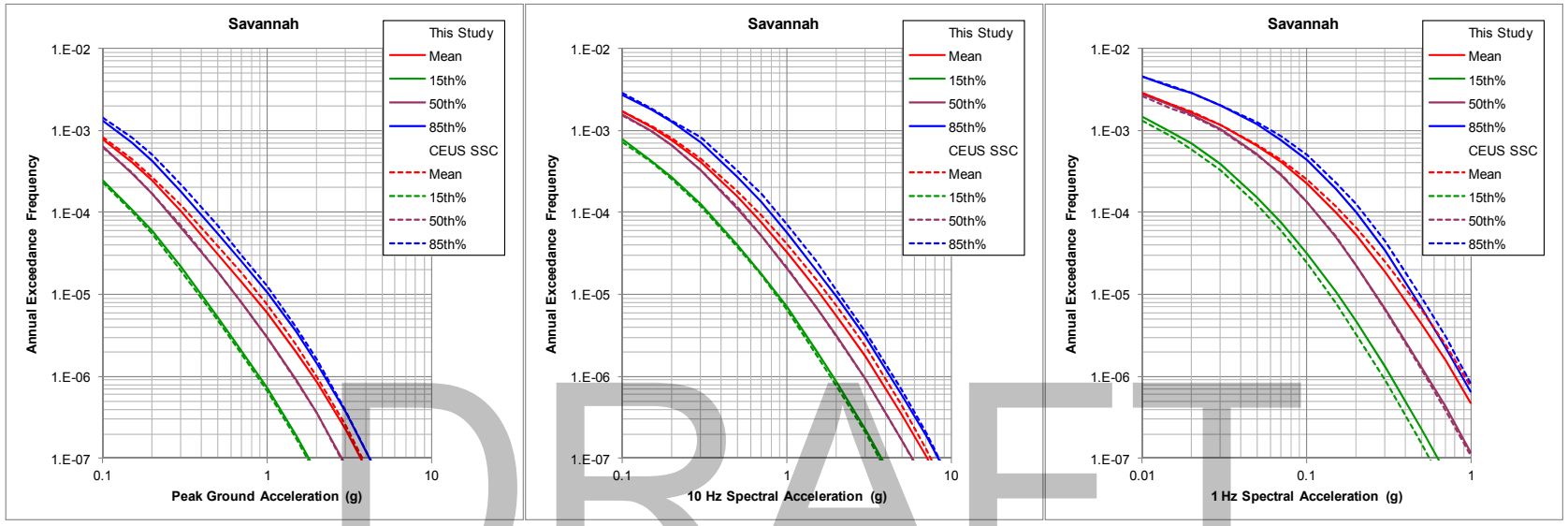

Figure 2.5.2-330: Comparison of hazard curves computed using AMEC E&I software with those listed in Chapter 8 of NUREG-2115 for the Savannah demonstration site

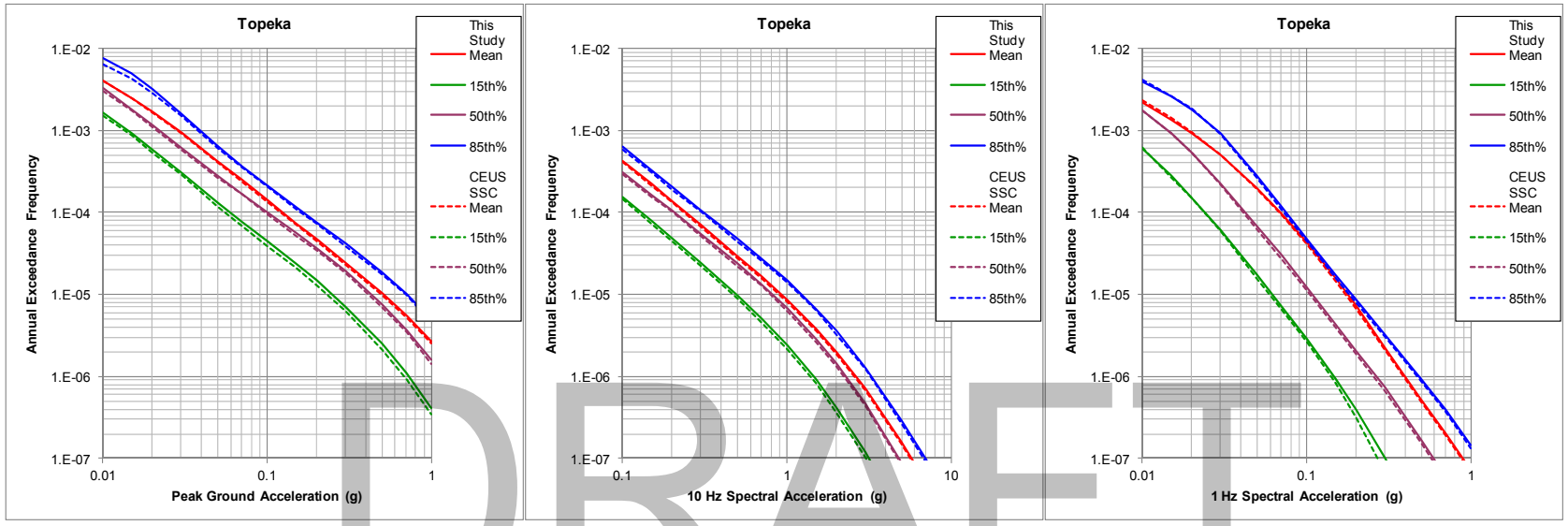

Figure 2.5.2-331: Comparison of hazard curves computed using AMEC E&I software with those listed in Chapter 8 of NUREG-2115 for the Topeka demonstration site

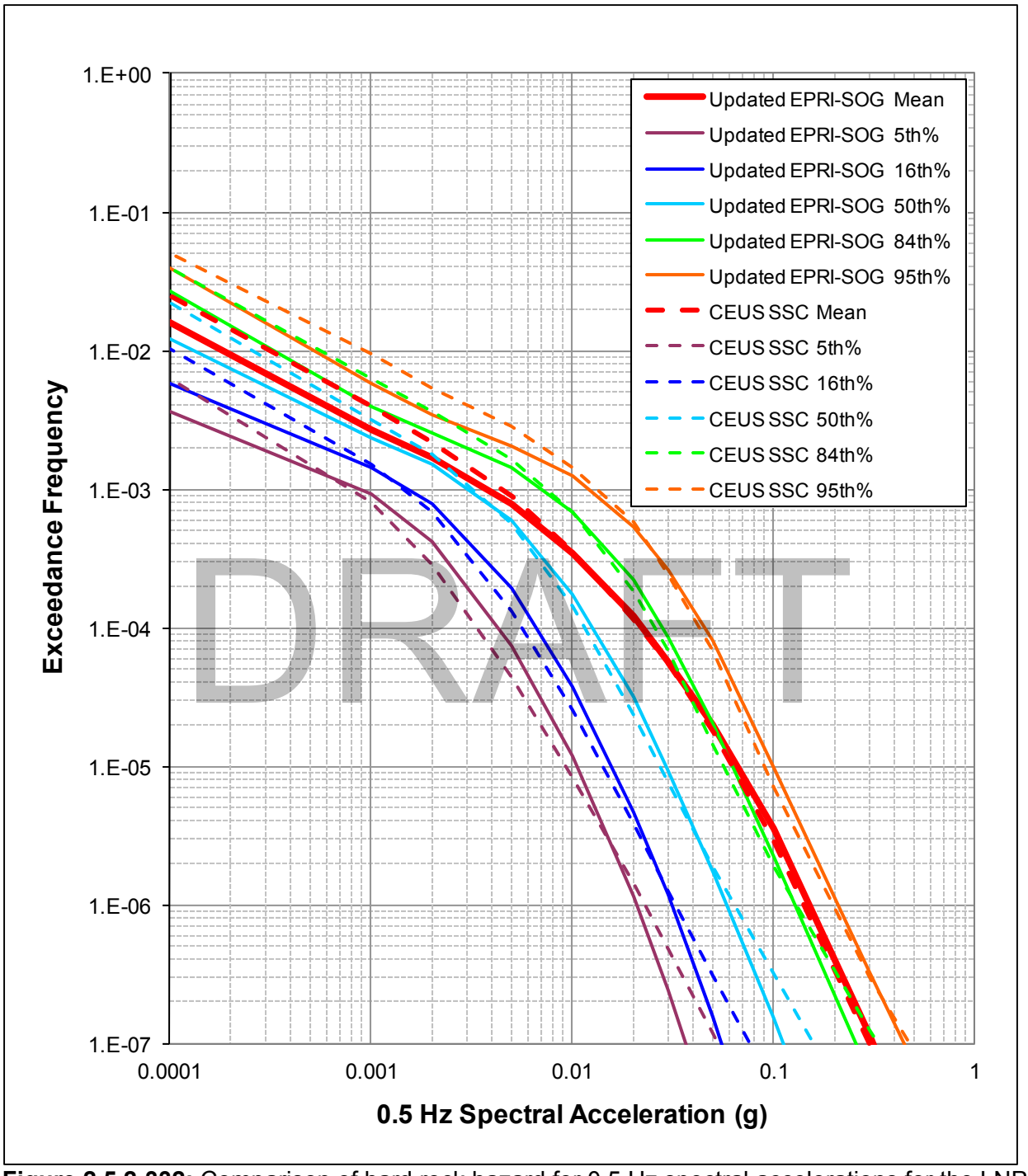

Figure 2.5.2-332: Comparison of hard rock hazard for 0.5 Hz spectral accelerations for the LNP Site computed using updated EPRI-SOG model with those obtained using the CEUS SSC model.

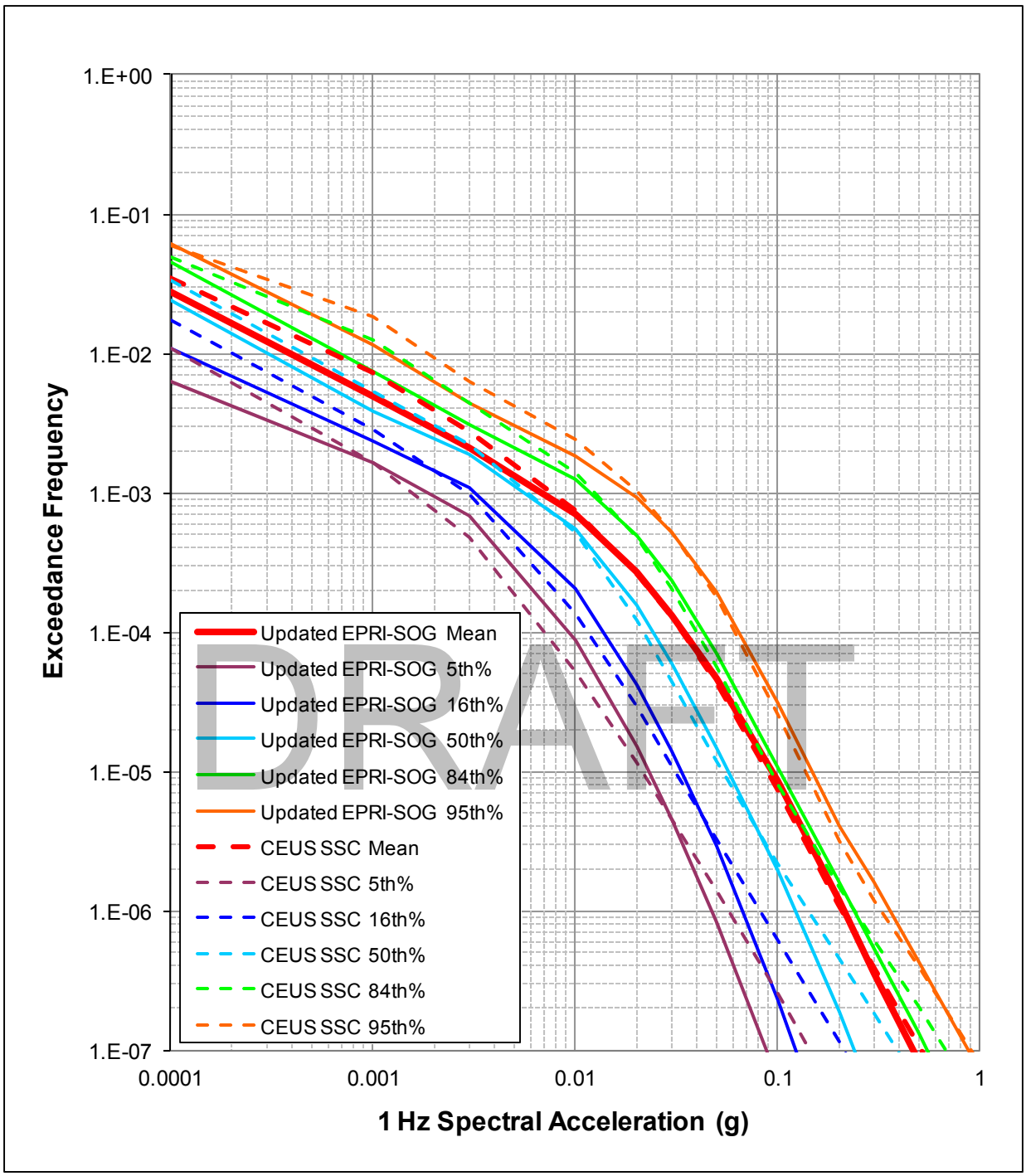

Figure 2.5.2-333: Comparison of hard rock hazard for 1 Hz spectral accelerations for the LNP Site computed using updated EPRI-SOG model with those obtained using the CEUS SSC model.

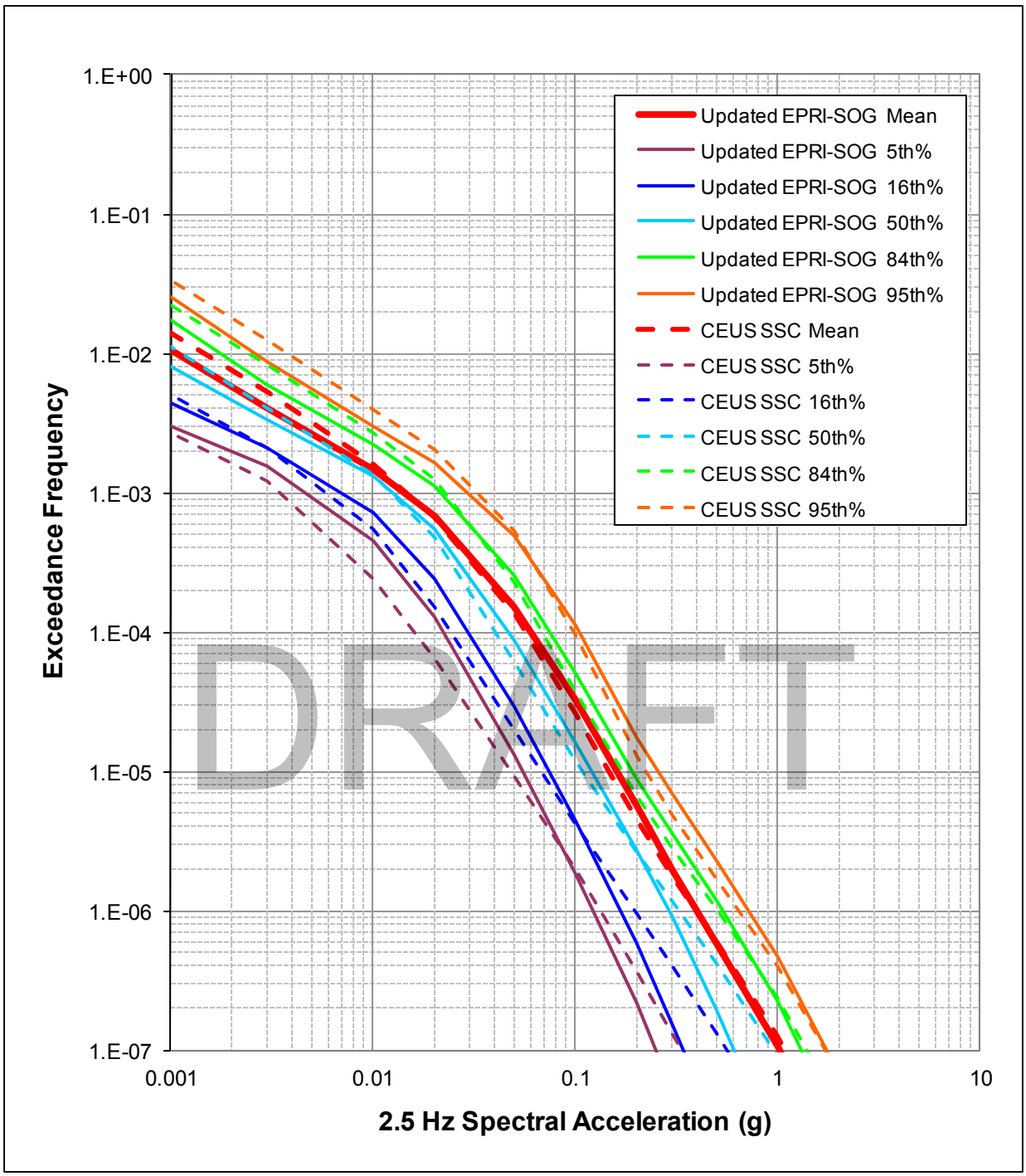

Figure 2.5.2-334: Comparison of hard rock hazard for 2.5 Hz spectral accelerations for the LNP Site computed using updated EPRI-SOG model with those obtained using the CEUS SSC model.

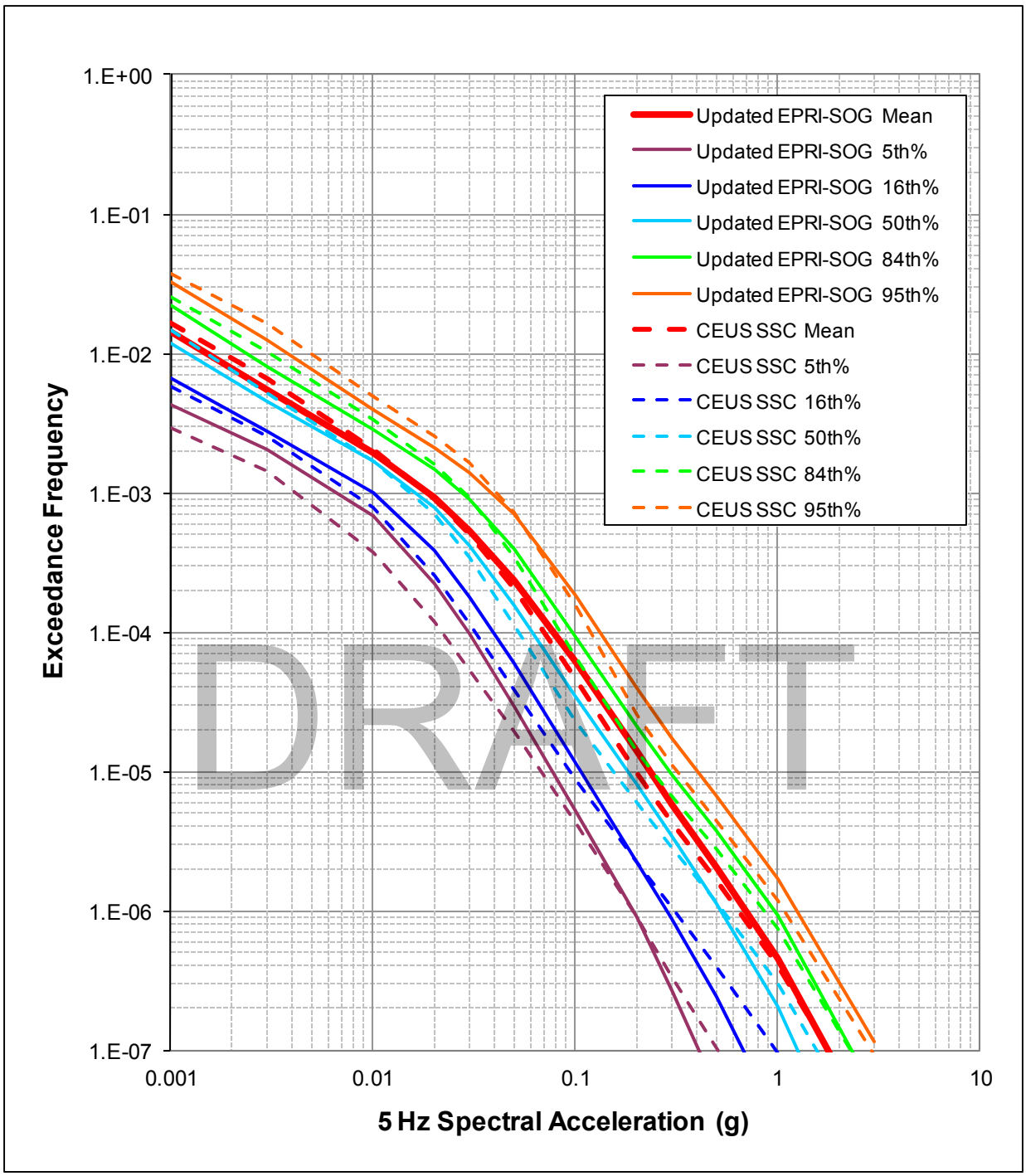

Figure 2.5.2-335: Comparison of hard rock hazard for 5 Hz spectral accelerations for the LNP Site computed using updated EPRI-SOG model with those obtained using the CEUS SSC model.

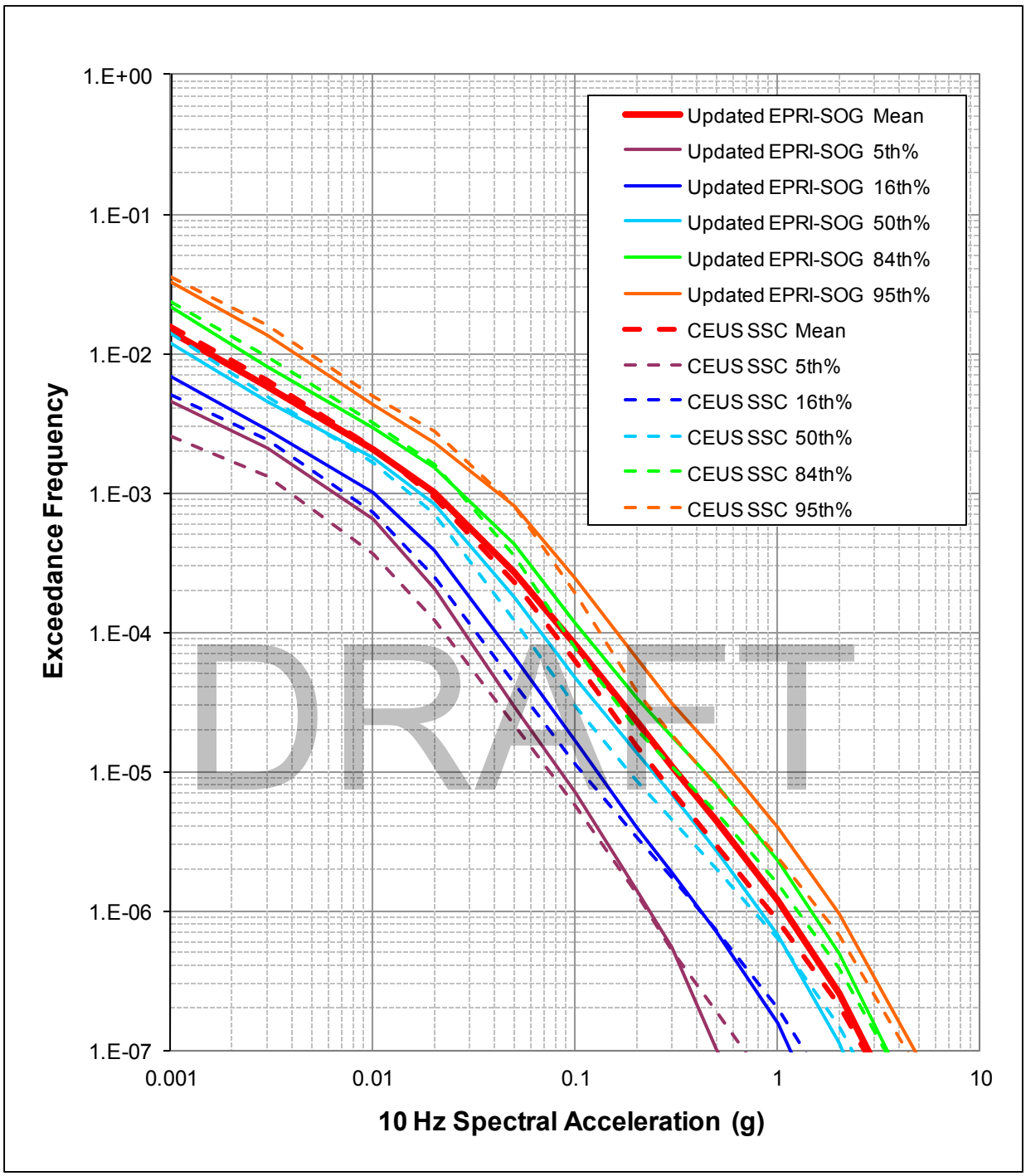

Figure 2.5.2-336: Comparison of hard rock hazard for 10 Hz spectral accelerations for the LNP Site computed using updated EPRI-SOG model with those obtained using the CEUS SSC model.

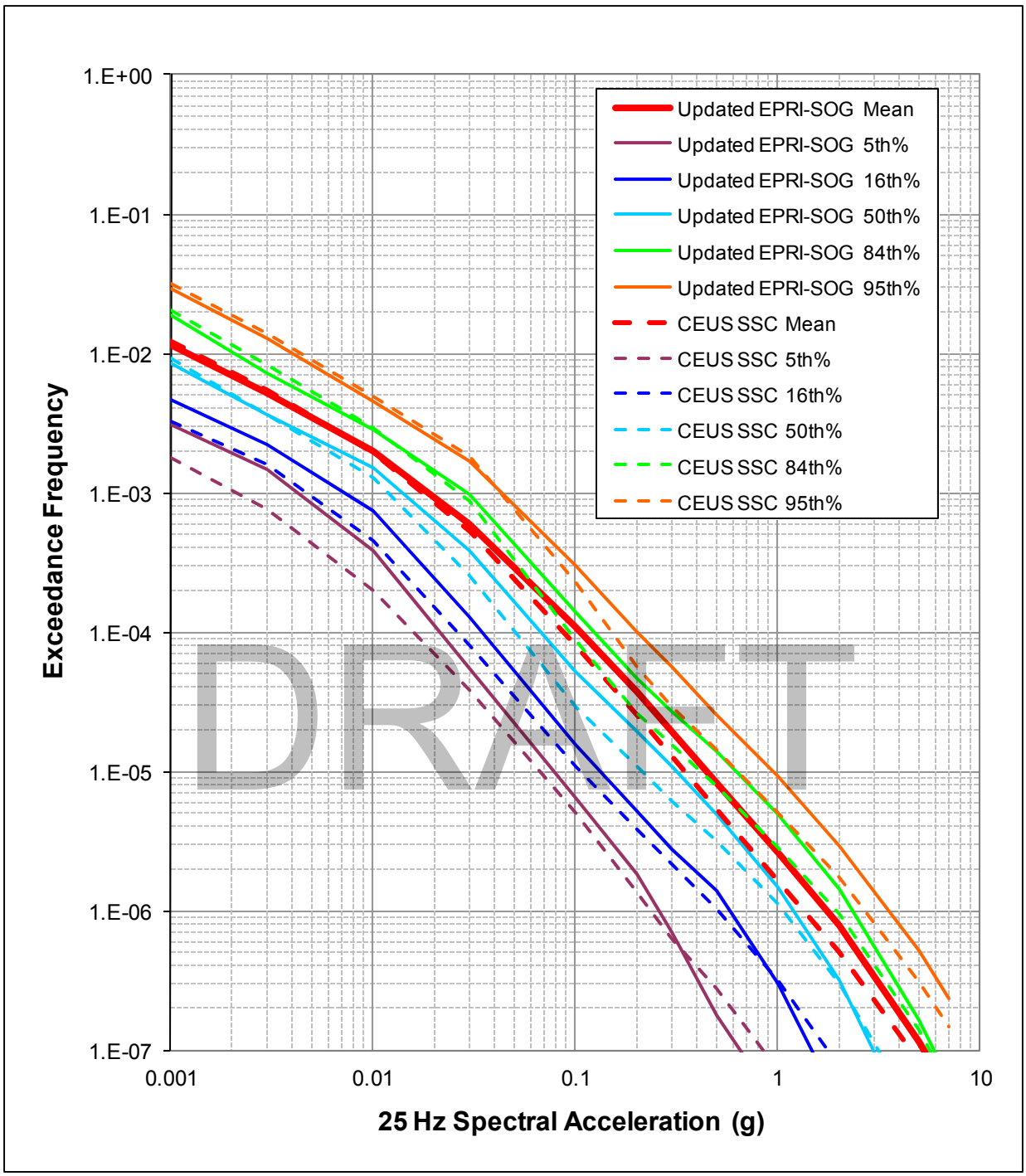

Figure 2.5.2-337: Comparison of hard rock hazard for 25 Hz spectral accelerations for the LNP Site computed using updated EPRI-SOG model with those obtained using the CEUS SSC model.

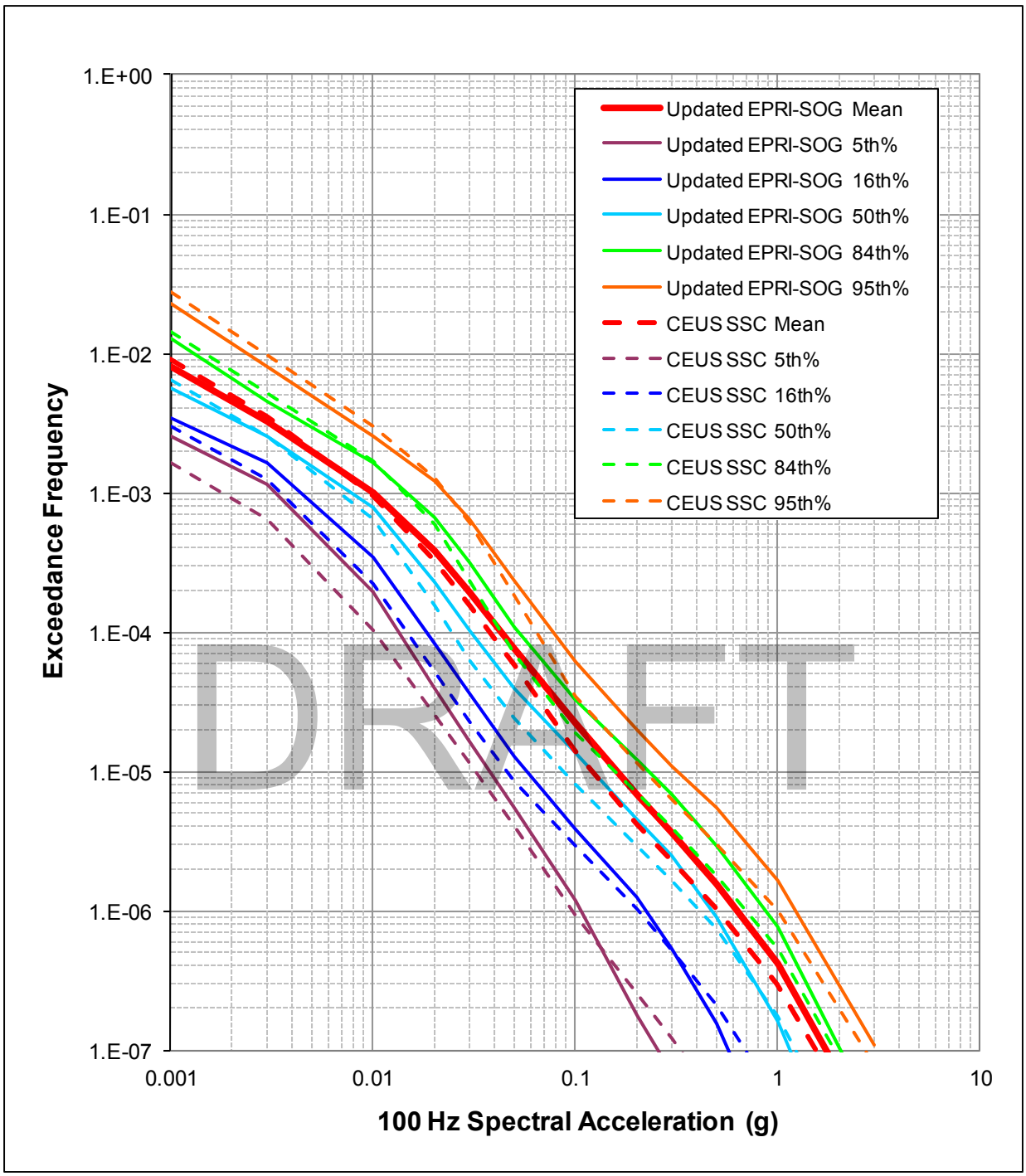

Figure 2.5.2-338: Comparison of hard rock hazard for 100 Hz spectral accelerations (PGA) for the LNP Site computed using updated EPRI-SOG model with those obtained using the CEUS SSC model.

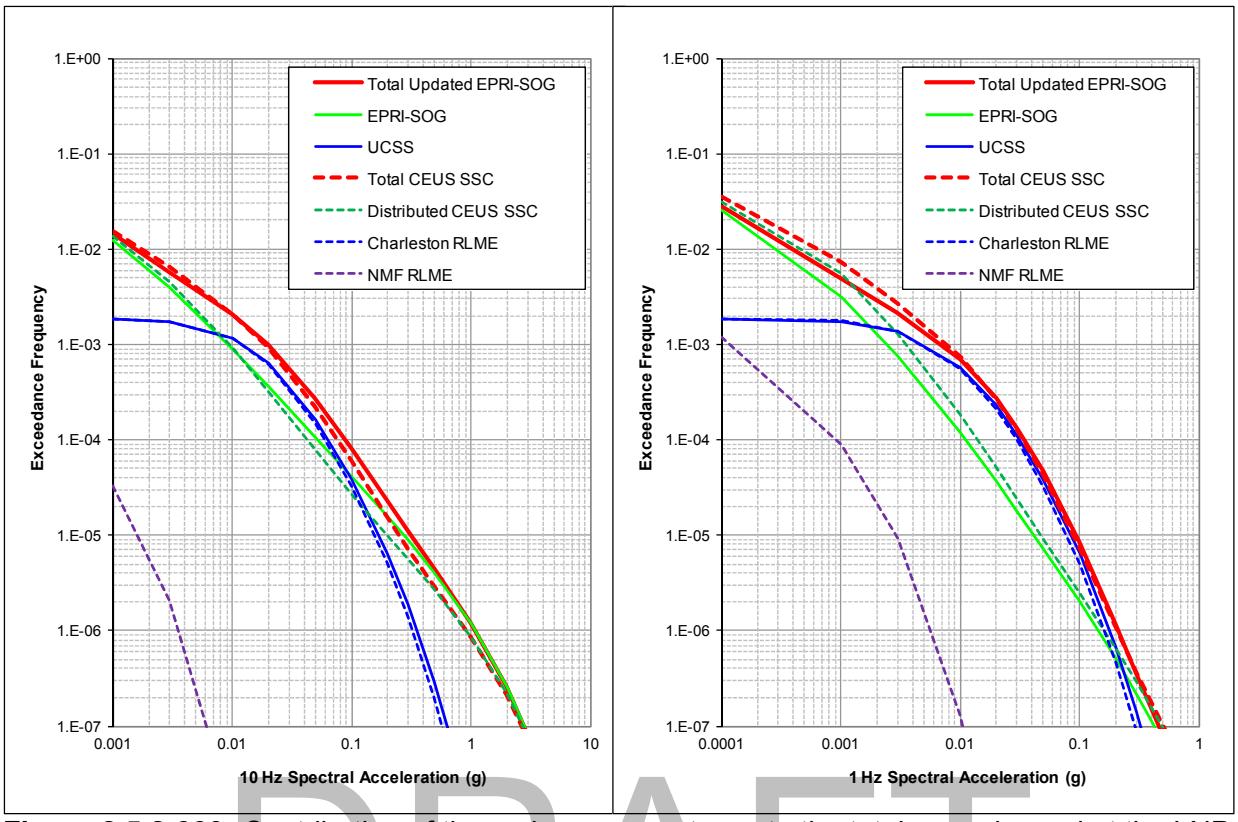

Figure 2.5.2-339: Contribution of the various source types to the total mean hazard at the LNP Site.

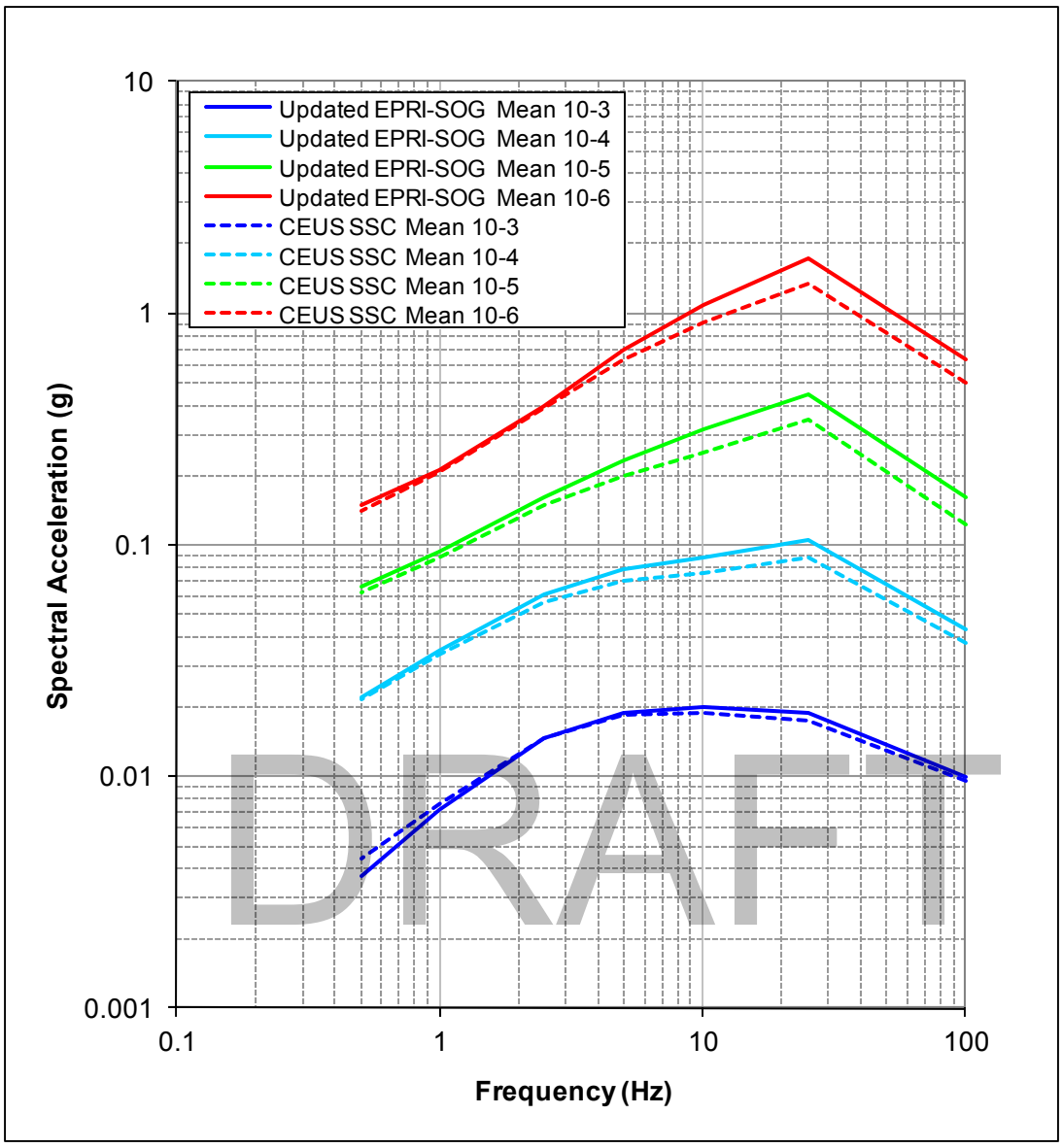

Figure 2.5.2-340: Comparison of hard rock UHRS based on updated EPRI-SOG model with results computed using the CEUS SSC model.

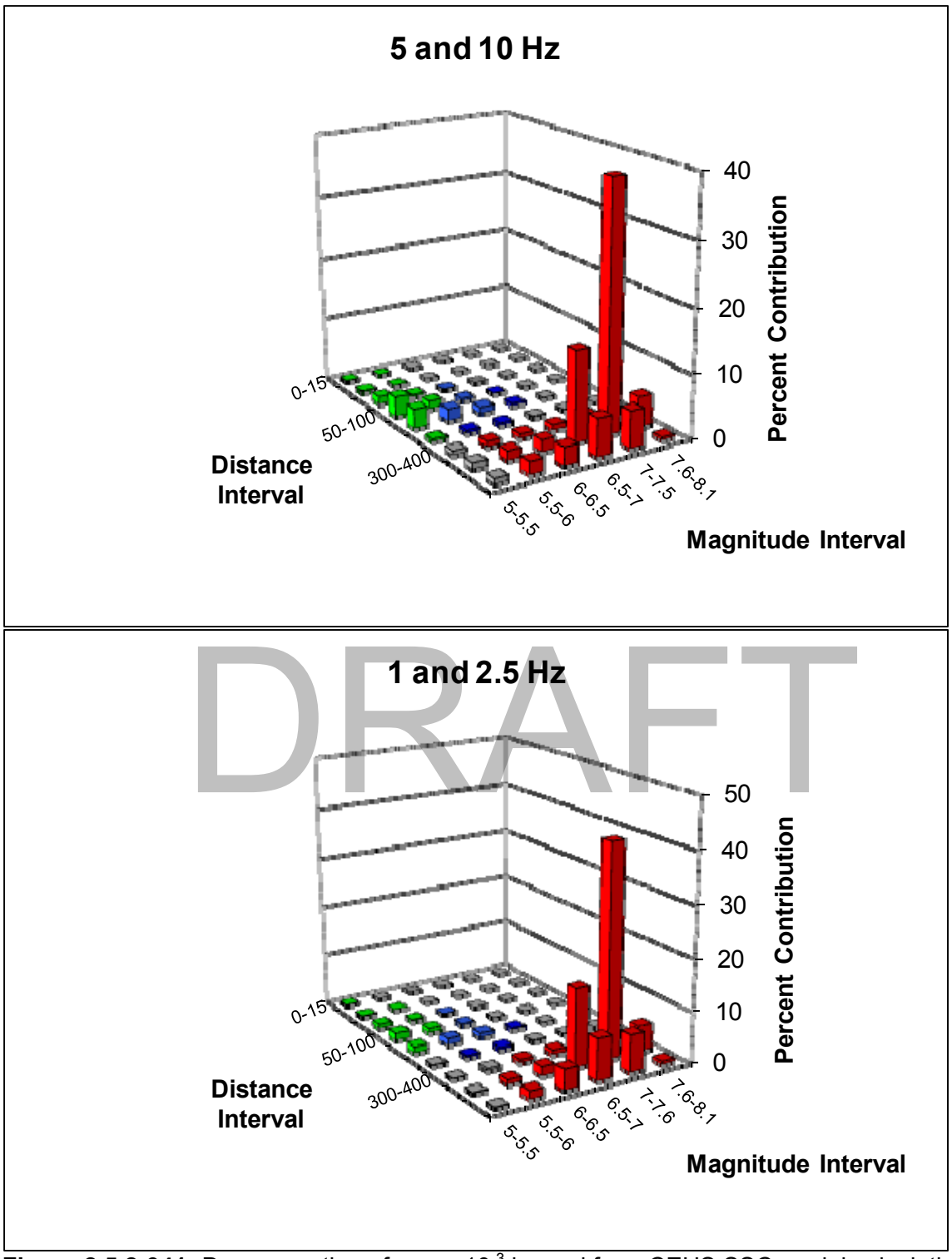

Figure 2.5.2-341: Deaggregation of mean 10^{-3} hazard from CEUS SSC model calculations.

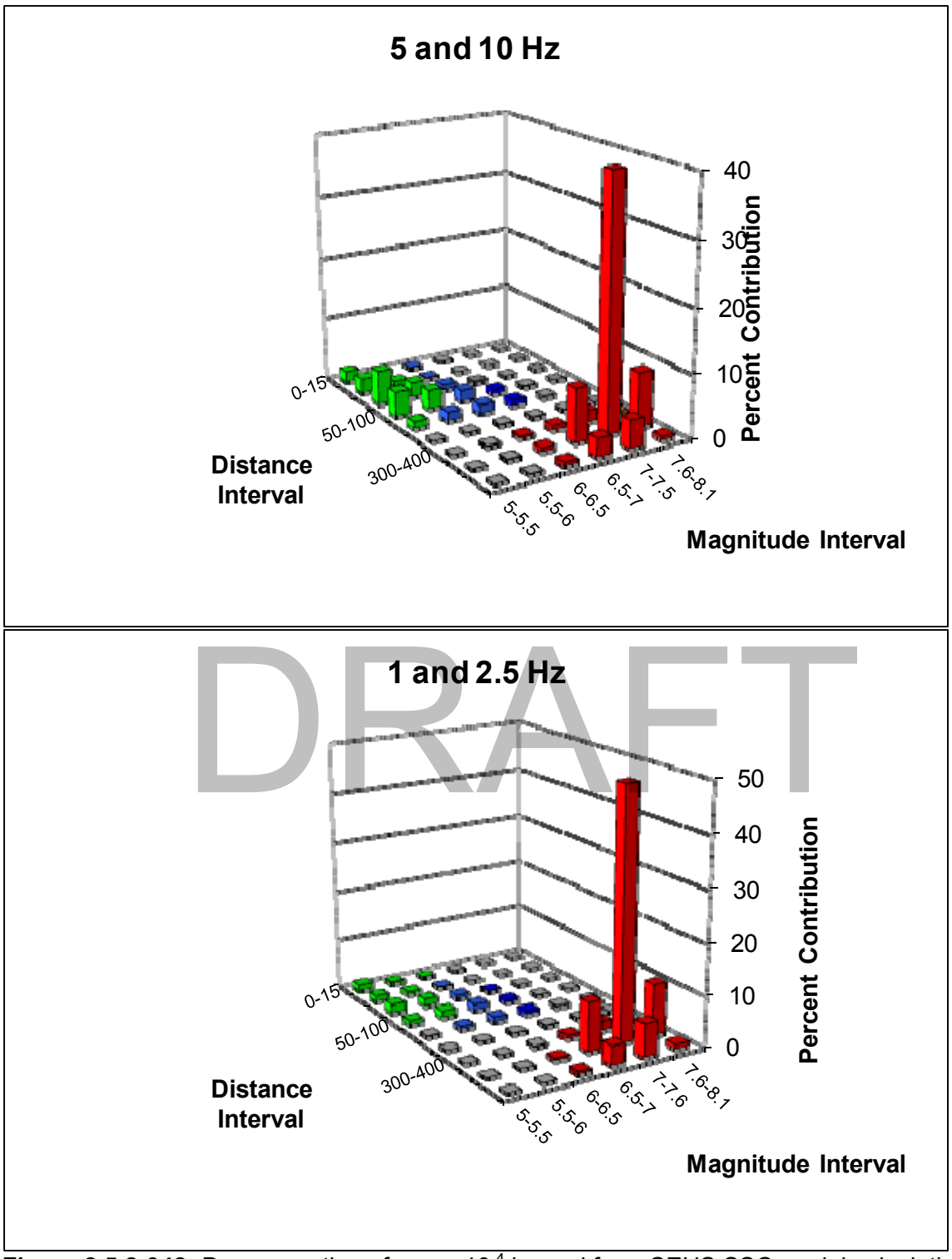

Figure 2.5.2-342: Deaggregation of mean 10^{-4} hazard from CEUS SSC model calculations.

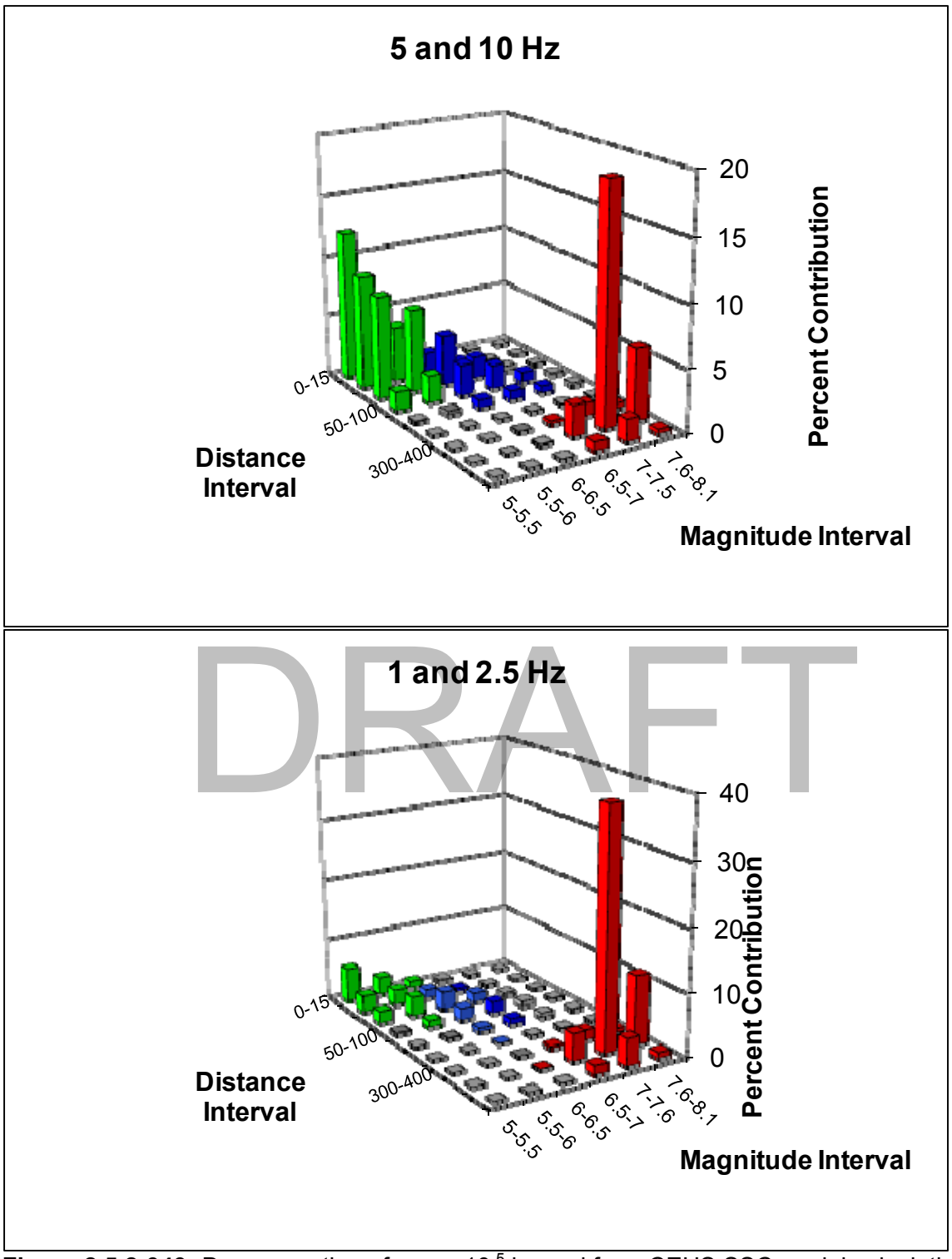

Figure 2.5.2-343: Deaggregation of mean 10^{-5} hazard from CEUS SSC model calculations.

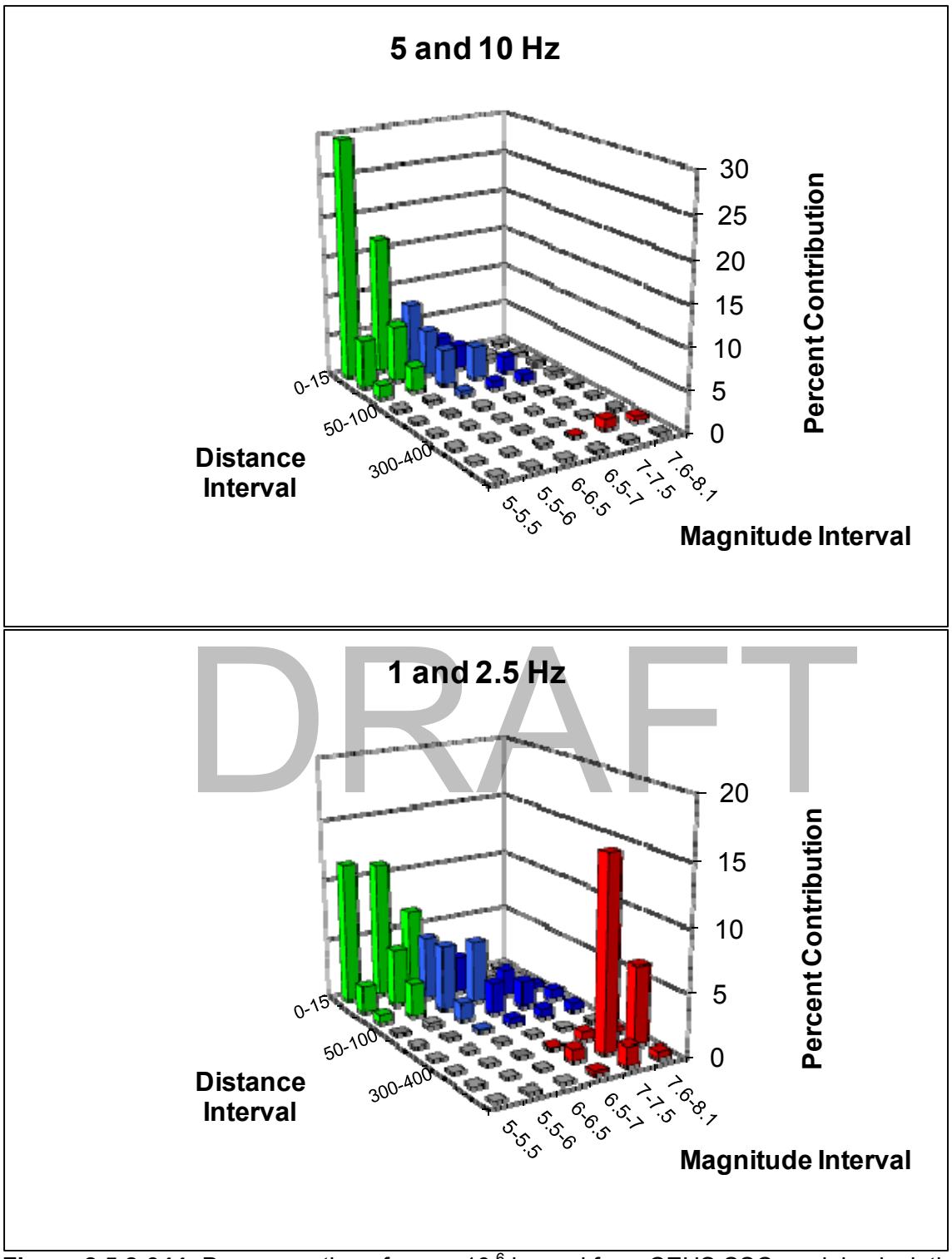

Figure 2.5.2-344: Deaggregation of mean 10^{-6} hazard from CEUS SSC model calculations.

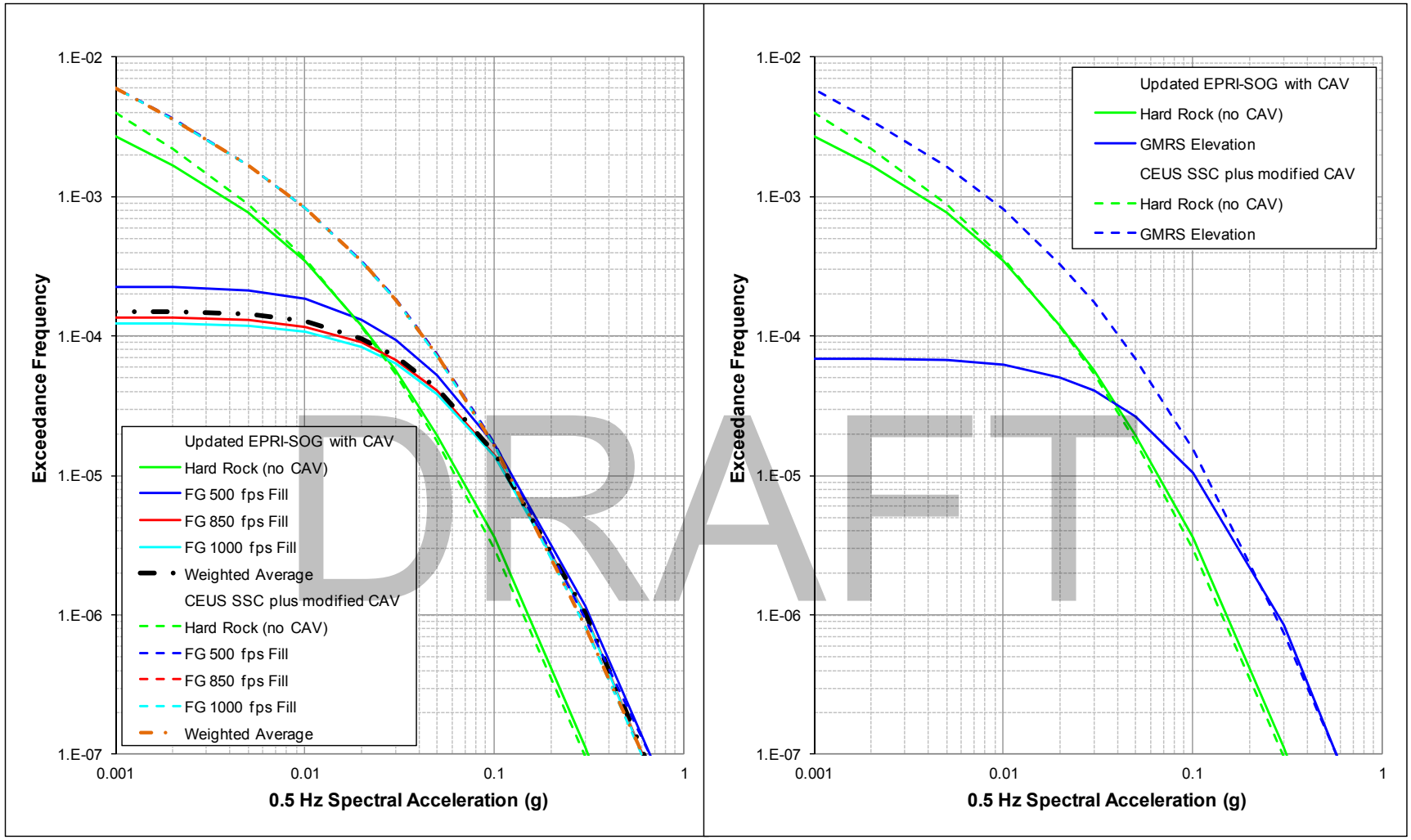

Figure 2.5.2-345: Comparison of mean hazard curves for 0.5 Hz spectral acceleration computed with CAV for the finished grade elevation (left) and the GMRS elevation (right). Solid lines are results for the updated EPRI-SOG model with CAV applied to all magnitudes and dashed lines are for the CEUS SSC model with CAV applies only to magnitudes < **M** 5.5.

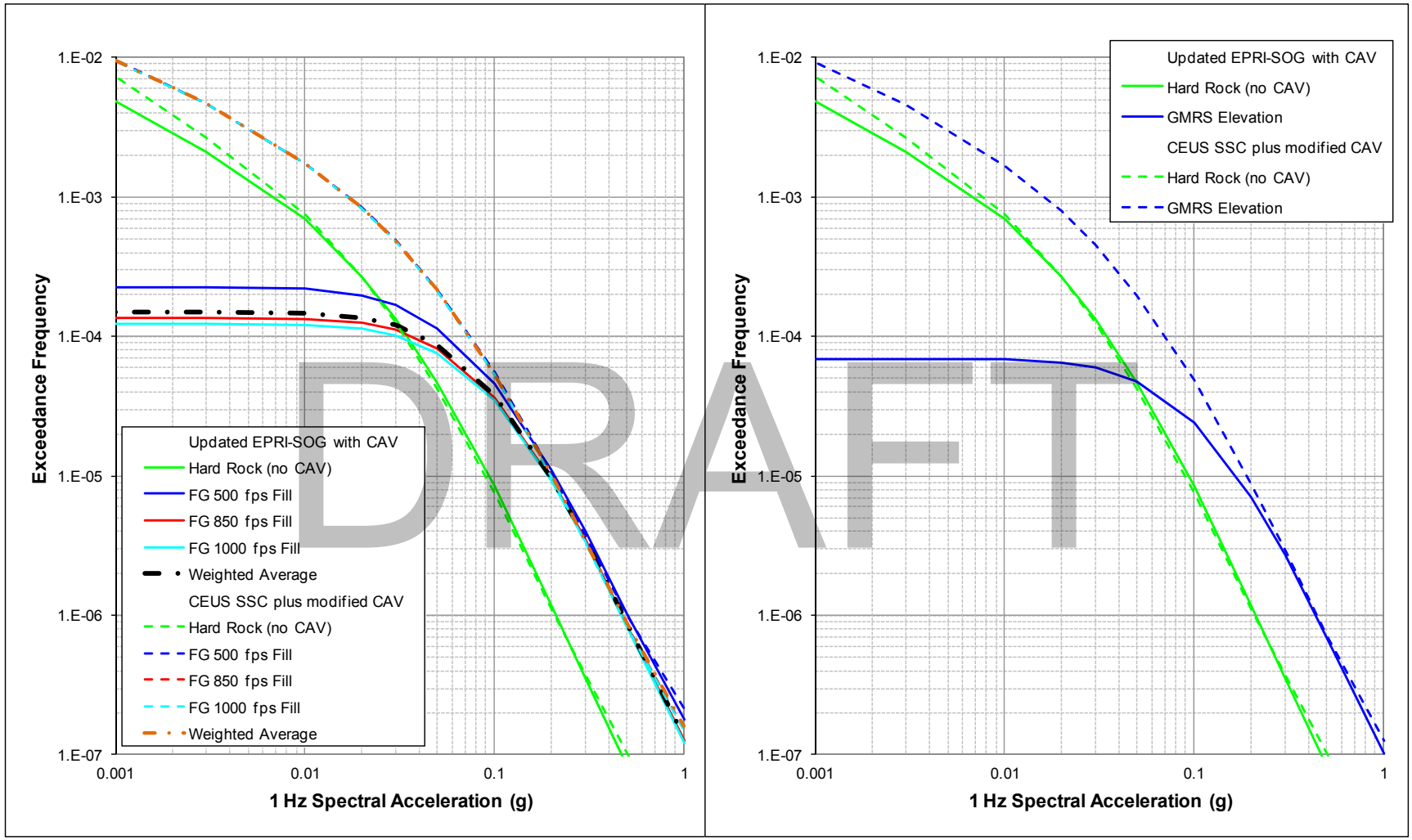

Figure 2.5.2-346: Comparison of mean hazard curves for 1 Hz spectral acceleration computed with CAV for the finished grade elevation (left) and the GMRS elevation (right). Solid lines are results for the updated EPRI-SOG model with CAV applied to all magnitudes and dashed lines are for the CEUS SSC model with CAV applies only to magnitudes < **M** 5.5.

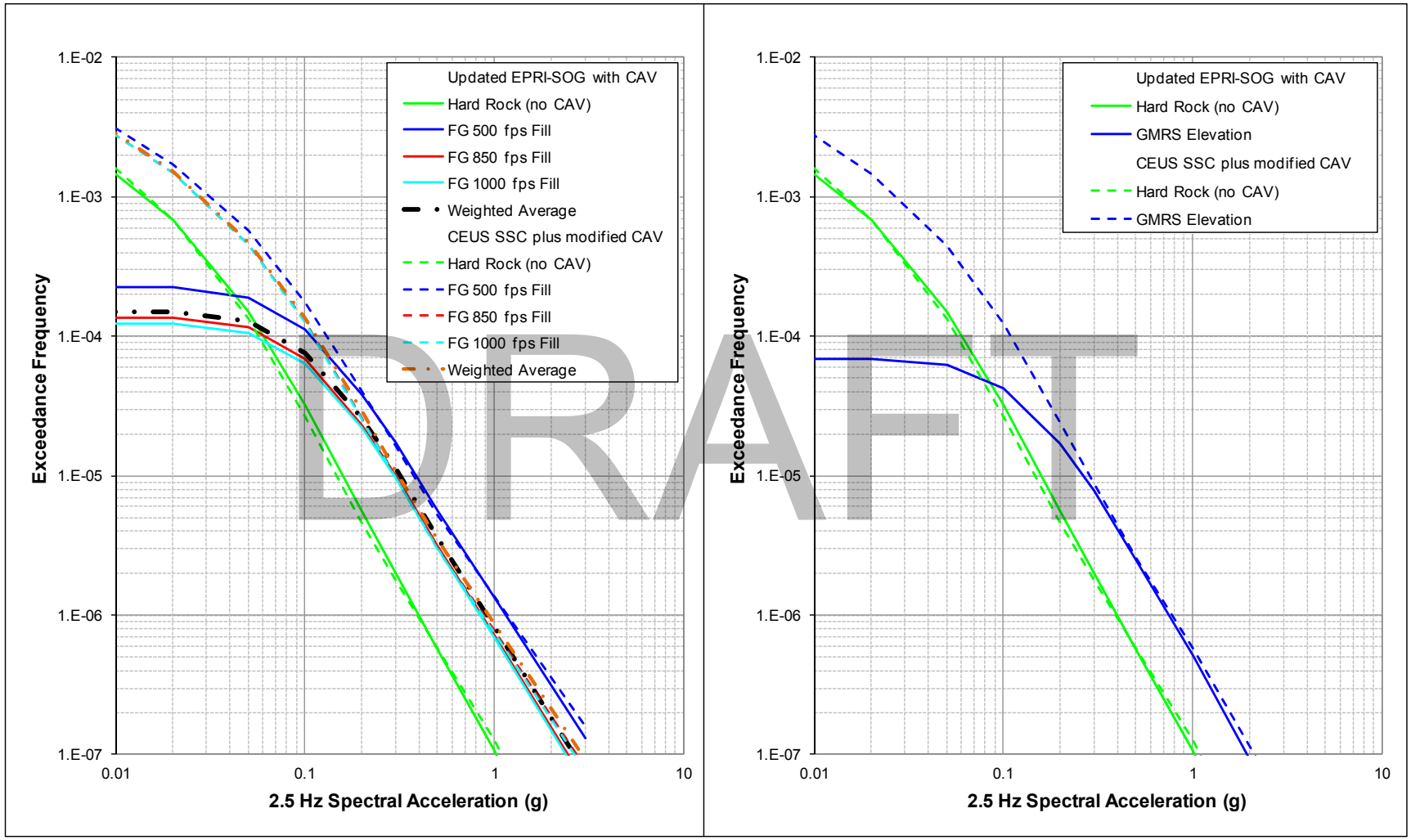

Figure 2.5.2-347: Comparison of mean hazard curves for 2.5 Hz spectral acceleration computed with CAV for the finished grade elevation (left) and the GMRS elevation (right). Solid lines are results for the updated EPRI-SOG model with CAV applied to all magnitudes and dashed lines are for the CEUS SSC model with CAV applies only to magnitudes < **M** 5.5.

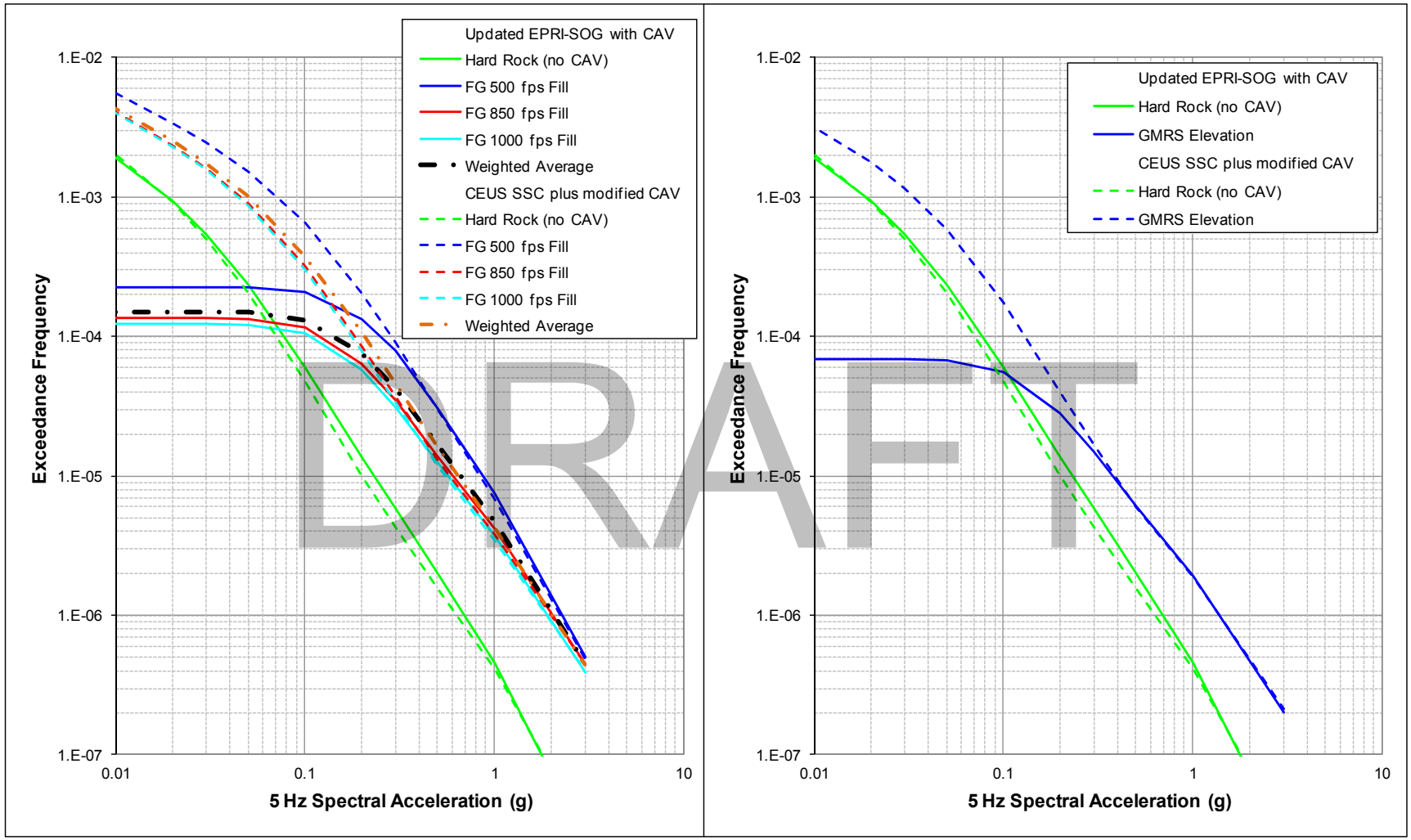

Figure 2.5.2-348: Comparison of mean hazard curves for 5 Hz spectral acceleration computed with CAV for the finished grade elevation (left) and the GMRS elevation (right). Solid lines are results for the updated EPRI-SOG model with CAV applied to all magnitudes and dashed lines are for the CEUS SSC model with CAV applies only to magnitudes < **M** 5.5.

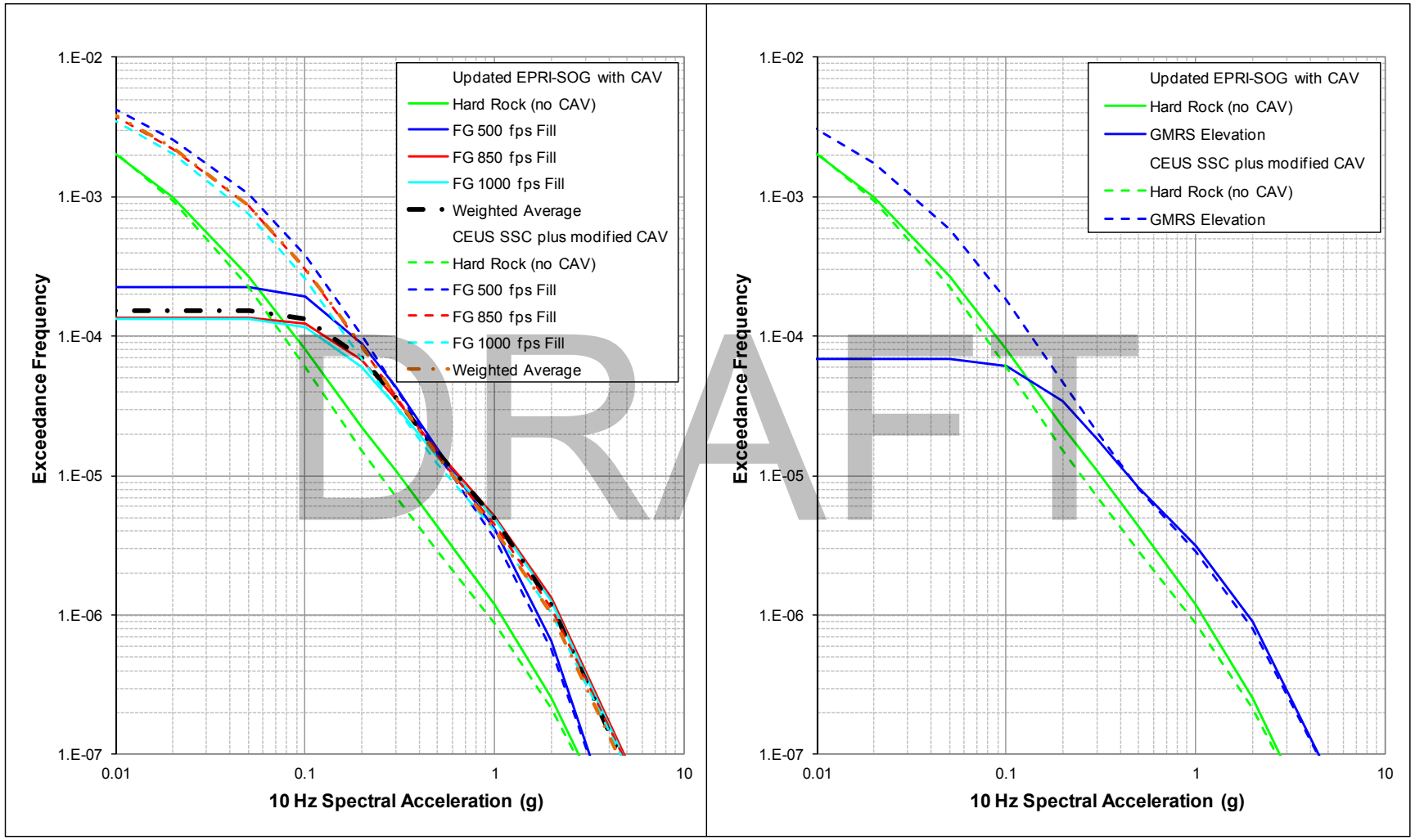

Figure 2.5.2-349: Comparison of mean hazard curves for 10 Hz spectral acceleration computed with CAV for the finished grade elevation (left) and the GMRS elevation (right). Solid lines are results for the updated EPRI-SOG model with CAV applied to all magnitudes and dashed lines are for the CEUS SSC model with CAV applies only to magnitudes < **M** 5.5.

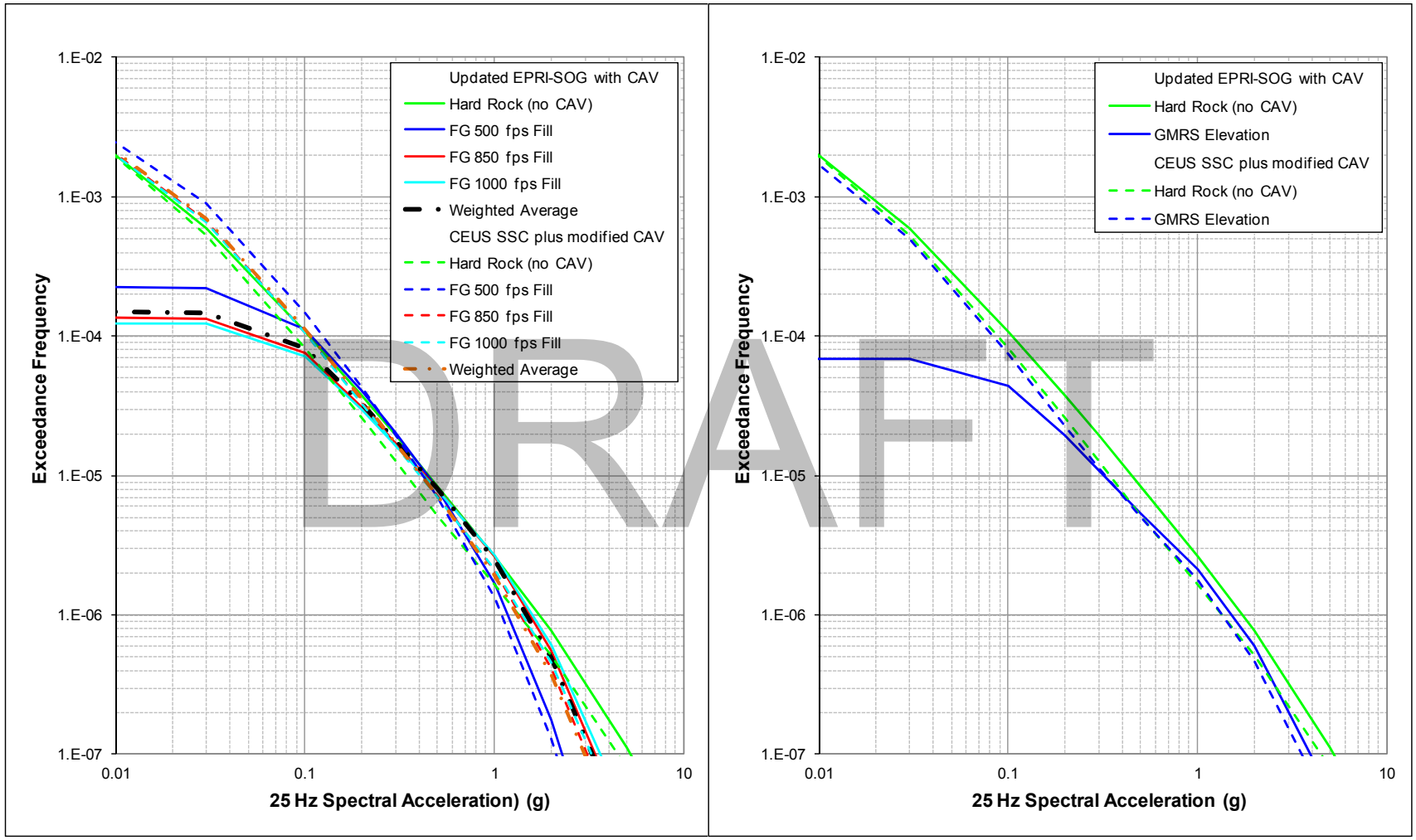

Figure 2.5.2-350: Comparison of mean hazard curves for 25 Hz spectral acceleration computed with CAV for the finished grade elevation (left) and the GMRS elevation (right). Solid lines are results for the updated EPRI-SOG model with CAV applied to all magnitudes and dashed lines are for the CEUS SSC model with CAV applies only to magnitudes < **M** 5.5.

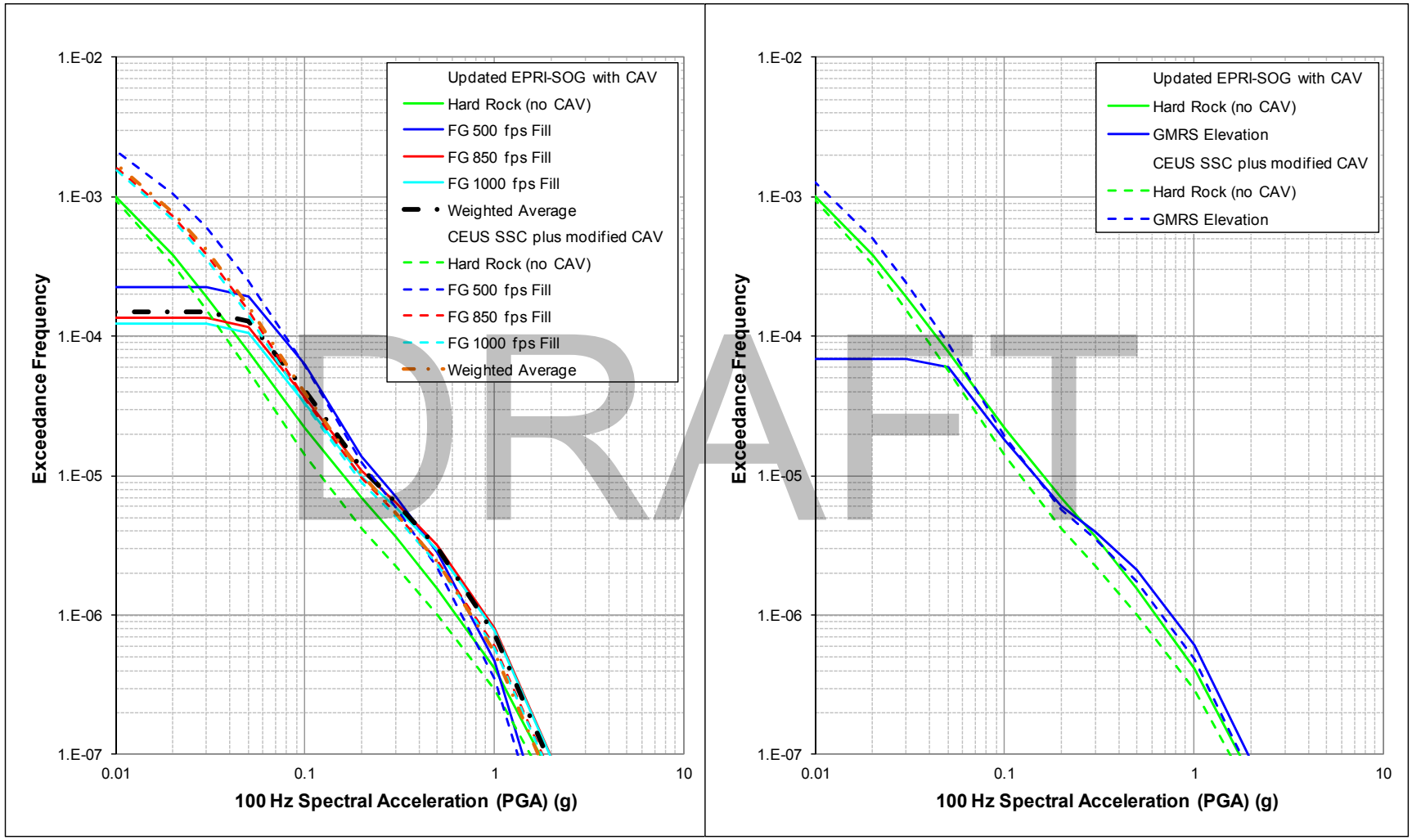

Figure 2.5.2-351: Comparison of mean hazard curves for 100 Hz spectral acceleration computed with CAV for the finished grade elevation (left) and the GMRS elevation (right). Solid lines are results for the updated EPRI-SOG model with CAV applied to all magnitudes and dashed lines are for the CEUS SSC model with CAV applies only to magnitudes < **M** 5.5.

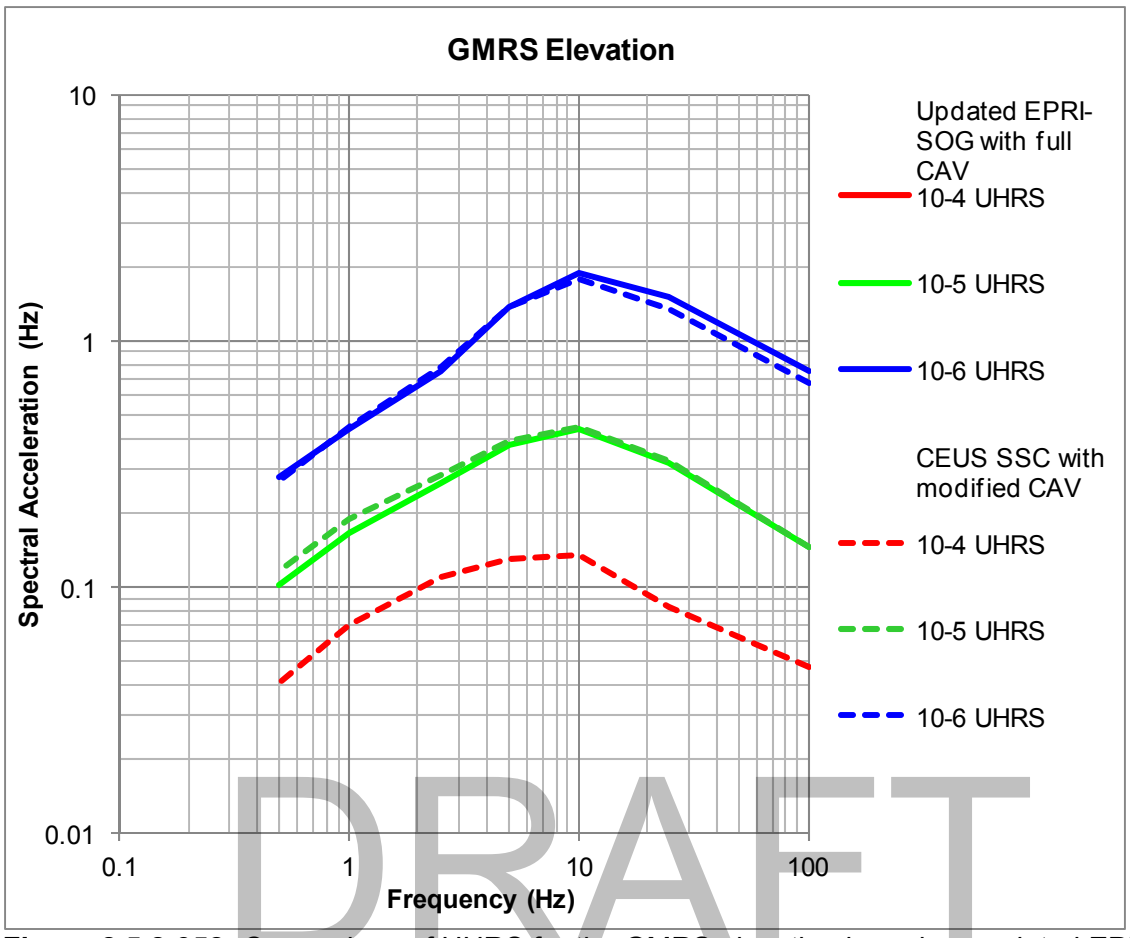

Figure 2.5.2-352: Comparison of UHRS for the GMRS elevation based on updated EPRI-SOG model with full CAV and the CEUS SSC model with modified CAV.

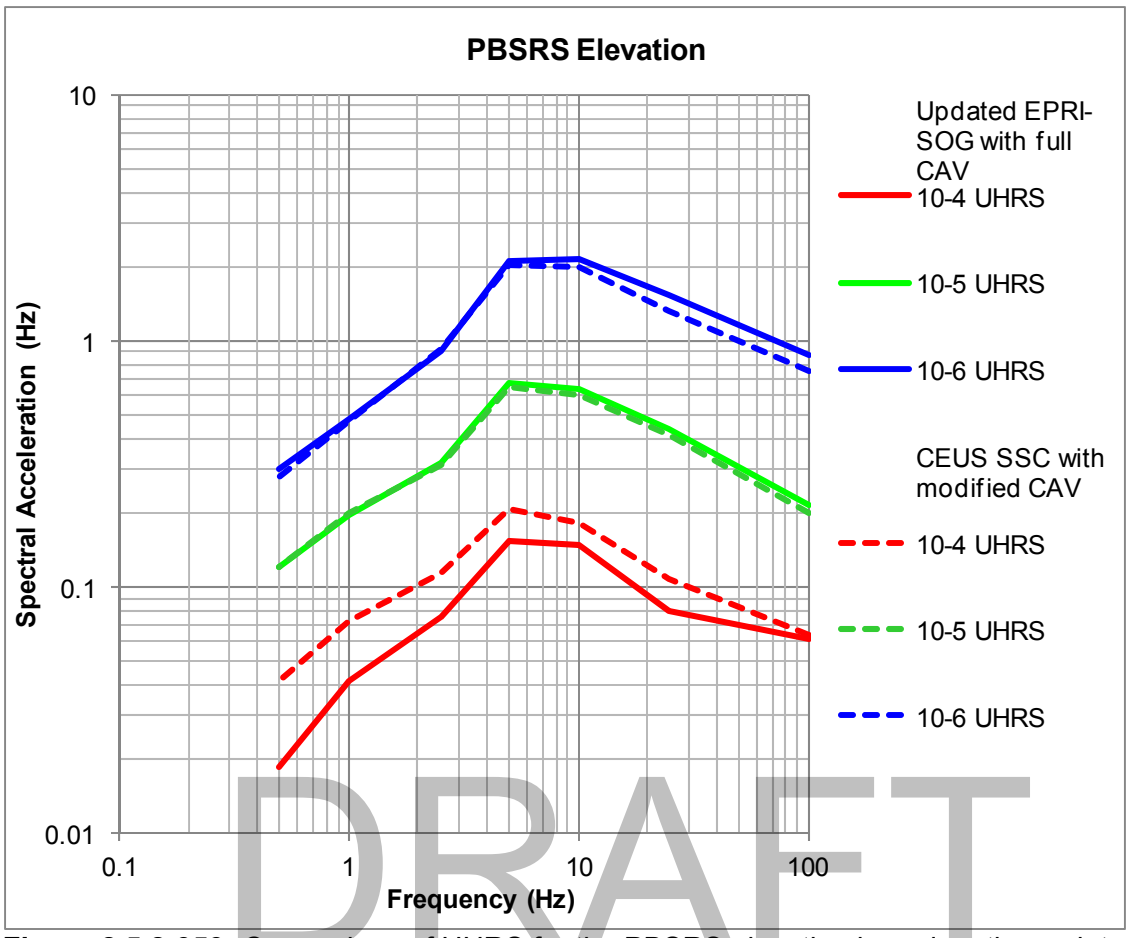

Figure 2.5.2-353: Comparison of UHRS for the PBSRS elevation based on the updated EPRI-SOG model with full CAV and the CEUS SSC model with modified CAV.

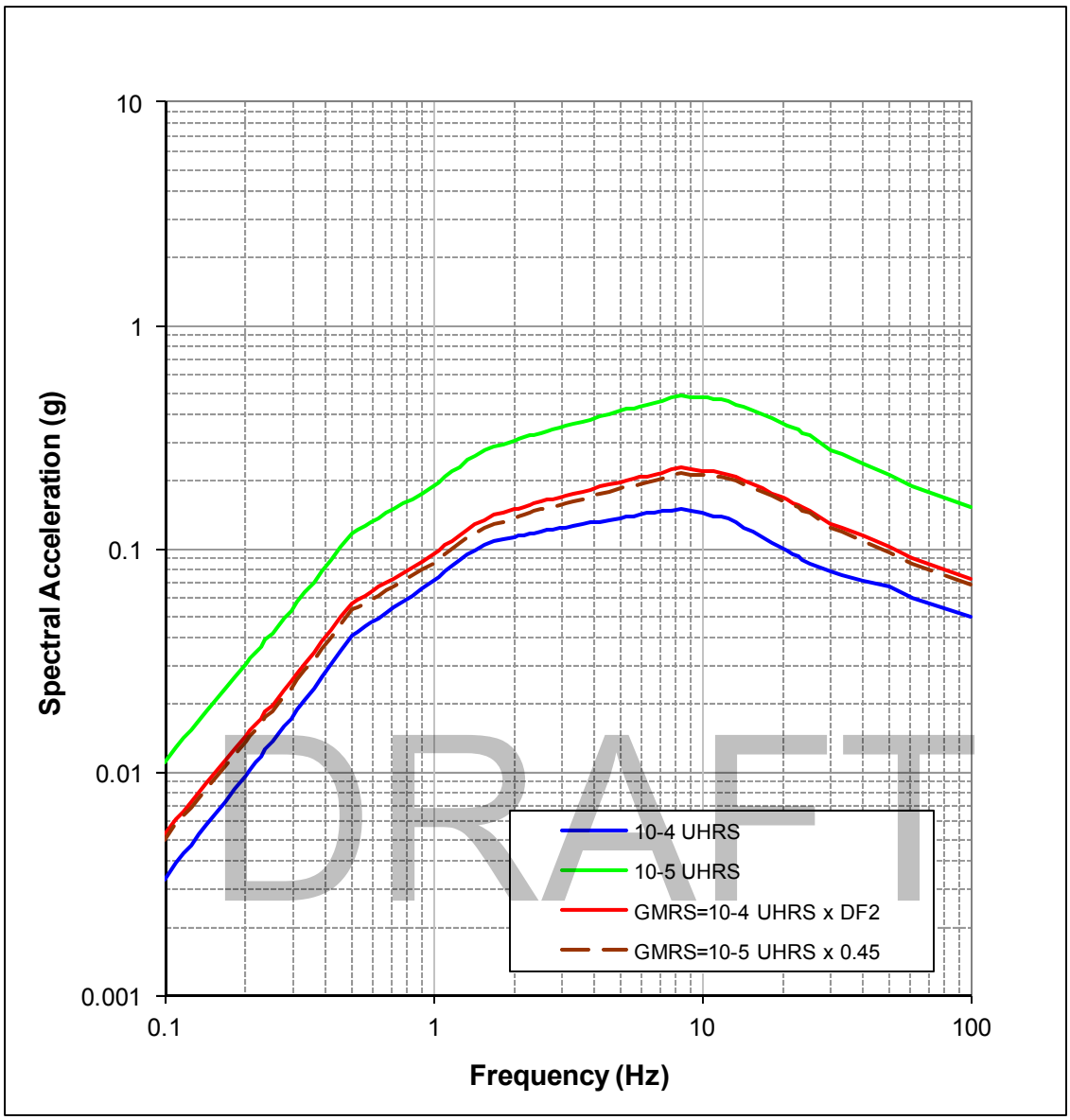

Figure 2.5.2-354: Development of horizontal GMRS based on the CEUS SSC model with modified CAV.

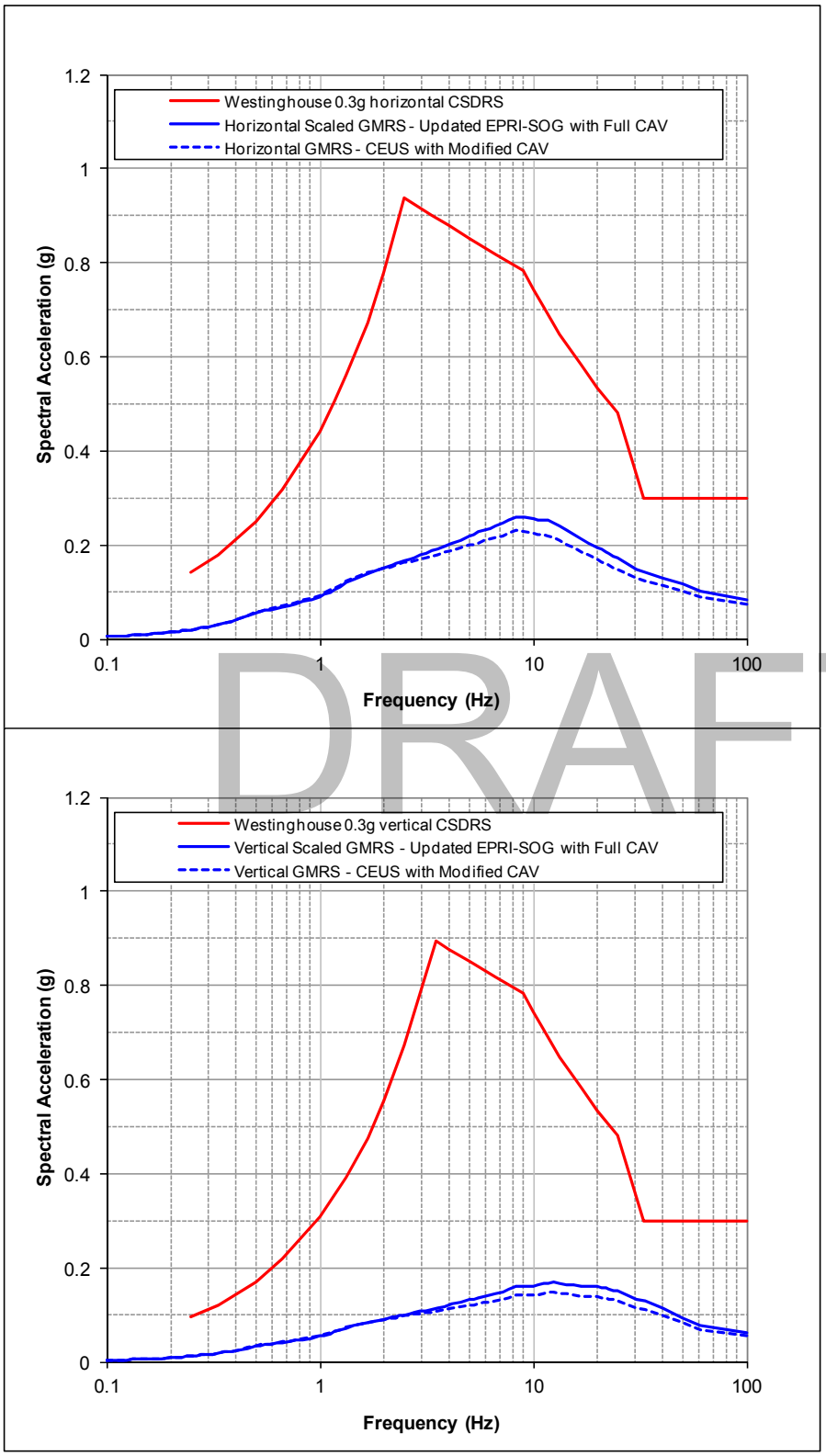

Figure 2.5.2-355 Comparison of GMRS based on updated EPRI-SOG and CEUS SSC models

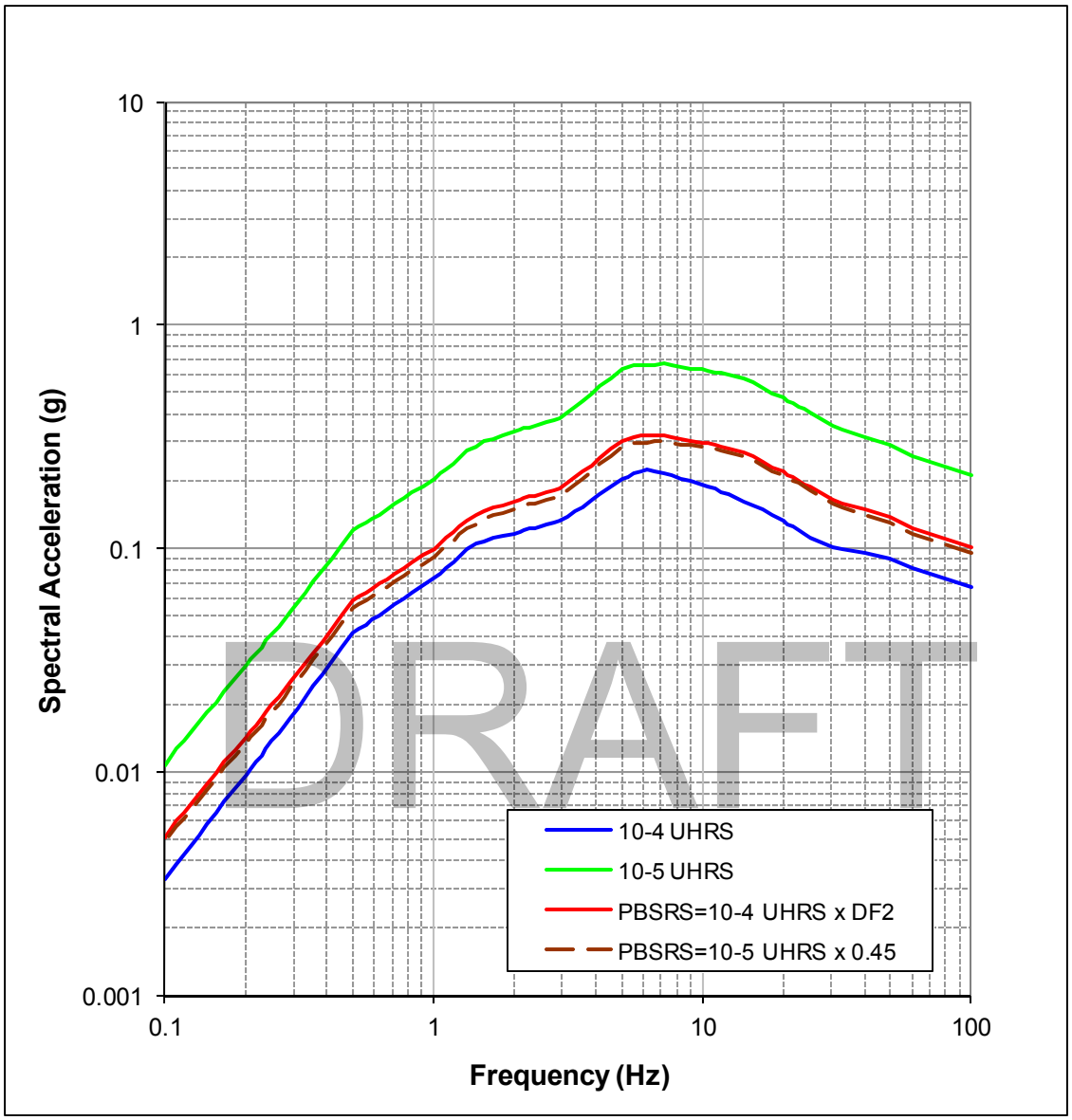

Figure 2.5.2-356: Development of horizontal PBSRS based on the CEUS SSC model with modified CAV.